Circulation Research

ORIGINAL RESEARCH

Immunometabolic Endothelial Phenotypes

Integrating Inflammation and Glucose Metabolism

Wusheng Xiao, William M. Oldham, Carmen Priolo, Arvind K. Pandey, Joseph Loscalzo

RATIONALE: Specific mechanisms linking inflammation and metabolic reprogramming—two hallmarks of many pathobiological processes—remain incompletely defined.

OBJECTIVE: To delineate the integrative regulatory actions governing inflammation and metabolism in endothelial cells.

METHODS AND RESULTS: Metabolomic profiling, glucose labeling and tracing, and Seahorse extracellular flux analyses revealed that the inflammatory mediators, TNFα (tumor necrosis factor alpha) and lipopolysaccharide, extensively reprogram cellular metabolism and particularly enhance glycolysis, mitochondrial oxidative phosphorylation (OXPHOS), and the pentose phosphate pathway in primary human arterial endothelial cells. Mechanistically, the enhancement in glycolysis and pentose phosphate pathway is mediated by activation of the NF-κB (nuclear factor-kappa B)–PFKFB3 (6-phosphofructo-2-kinase/fructose 2,6-bisphosphatase 3) axis and upregulation of G6PD (glucose 6-phosphate dehydrogenase), respectively, while enhanced OXPHOS was attributed to suppression of the FOXO1 (forkhead box O1)-PDK4 (pyruvate dehydrogenase kinase 4) axis. Restoration of the FOXO1-PDK4 axis attenuated the TNFα- or lipopolysaccharide-induced increase in OXPHOS but worsened inflammation in vitro, whereas enhancement of OXPHOS by pharmacological blockade of PDKs attenuated inflammation in mesenteric vessels of lipopolysaccharide-treated mice. Notably, suppression of *G6PD* expression or its activity potentiated the metabolic shift to glycolysis or endothelial inflammation, while inhibition of the NF-κB–PFKFB3 signaling, conversely, blunted the increased glycolysis or inflammation in in vitro and in vivo sepsis models.

CONCLUSIONS: These results indicate that inflammatory mediators modulate the metabolic fates of glucose and that stimulation of glycolysis promotes inflammation, whereas enhancement of OXPHOS and the pentose phosphate pathway suppresses inflammation in the endothelium. Characterization of these immunometabolic phenotypes may have implications for the pathogenesis and treatment of many cardiovascular diseases.

GRAPHIC ABSTRACT: A graphic abstract is available for this article.

Key Words: endothelial cells ■ glucose ■ glycolysis ■ inflammation ■ mitochondria

Editorial, see p 30 | In This Issue, see p 2 | Meet the First Author, see p 3

The endothelium—a monolayer of endothelial cells (ECs) lining the vasculature—is a dynamic, heterogeneous, and extensive structure that possesses vital secretory, synthetic, sensory, barrier, transport, metabolic, and immunologic functions.[1] Normally, ECs in adults are quiescent, which helps to maintain an anti-inflammatory, antithrombotic, and fibrinolytic microenvironment.[1] Maintaining such a niche requires that quiescent ECs produce a variety of vasoactive factors (eg, NO•),[2] for which reason they are expected to be metabolically active. Since ECs, particularly arterial ECs, are exposed to an oxygen-rich environment in normal vessels, it is reasonable to speculate that ECs rely on mitochondrial respiration for energy production. Surprisingly, mounting evidence suggests that glycolysis is the predominant glucose utilization pathway and contributes 75% to 85% of total cellular ATP levels in quiescent and proliferating ECs.[3–7] This metabolic feature of ECs maximizes the delivery of

Correspondence to: Joseph Loscalzo, MD, PhD, Department of Medicine, Brigham and Women's Hospital, 75 Francis St, Boston, MA 02115. Email jloscalzo@rics.bwh.harvard.edu

The Data Supplement is available with this article at https://www.ahajournals.org/doi/suppl/10.1161/CIRCRESAHA.120.318805.

For Sources of Funding and Disclosures, see page 27.

ORIGINAL RESEARCH

Novelty and Significance

What Is Known?

- Endothelial dysfunction contributes to the development of many cardiovascular pathobiologies and diseases.
- Inflammation and metabolic reprogramming are two hallmarks of numerous cardiovascular disorders.

What New Information Does This Article Contribute?

- Inflammatory stimuli extensively reprogram endothelial cell metabolism.
- Glucose metabolic pathways distinctly modulate endothelial inflammation in vitro and in vivo.
- Glycolysis is activated as a proinflammatory mechanism in endothelial cells, while mitochondrial oxidative phosphorylation and the pentose phosphate pathway are enhanced as homeostatic anti-inflammatory responses.

The interregulation of inflammation and metabolism in the endothelium remains incompletely defined. Here, we demonstrate that the immunometabolic phenotype of the endothelium is dynamic and adaptive and that endothelial cell metabolism is reprogrammed in response to inflammatory stimulation. Specifically, inflammatory stimuli activate all 3 central glucose metabolic pathways, glycolysis, mitochondrial oxidative phosphorylation, and the pentose phosphate pathway. Intriguingly, stimulation of glycolysis promotes inflammation, whereas enhancement of oxidative phosphorylation and the pentose phosphate pathway suppresses inflammation in vitro and in vivo. Knowledge gained from this study provides insight into fundamental mechanisms underlying immunometabolic interactions in a unique cell type essential to normal vascular function and to the vascular inflammatory response, and may offer a novel rationale for developing therapeutic metabolic strategies for the treatment of inflammatory vascular disorders.

Nonstandard Abbreviations and Acronyms

AoEC	aortic endothelial cell
CCL2	C-C motif chemokine ligand 2
EC	endothelial cell
ECAR	extracellular acidification rate
FOXO1	forkhead box O1
G6PD	glucose 6-phosphate dehydrogenase
GSH	glutathione
IκBα(DN)	dominant-negative IκBα protein
ICAM1	intercellular adhesion molecule 1
IKK2	IκB kinase 2
LAC	lactate
LPS	lipopolysaccharide
NF-κB	nuclear factor-kappa B
NOX4	NADPH oxidase 4
OCR	oxygen consumption rate
OXPHOS	oxidative phosphorylation
PAEC	pulmonary artery endothelial cell
PAH	pulmonary arterial hypertension
PDK4	pyruvate dehydrogenase kinase 4
PFKFB3	6-phosphofructo-2-kinase/fructose 2,6-bisphosphatase 3
PI3K	phosphatidylinositol 3-kinase
PKM2	PYR kinase M2
PPP	pentose phosphate pathway
PYR	pyruvate
RNA-seq	RNA sequencing
TCA	tricarboxylic acid
TNFα	tumor necrosis factor alpha
VCAM1	vascular cell adhesion molecule 1

oxygen to perivascular cells and tissues and minimizes the production of reactive oxygen species through mitochondrial oxidative phosphorylation (OXPHOS).[7,8]

The endothelium is also the first line of defense against inflammatory insults in the vasculature. With inflammatory stimulation, quiescent ECs are activated to produce proinflammatory molecules and reactive oxygen species.[1,9] These cellular and molecular events disrupt vascular integrity and facilitate the adherence and transendothelial migration of circulating leukocytes, all of which create an inflammatory, prothrombotic, and antifibrinolytic microenvironment, and promote metabolic alterations in ECs.[1,9] Inflammation and metabolic alterations have been inextricably linked to the development of numerous cardiovascular diseases, such as atherosclerosis and pulmonary arterial hypertension (PAH).[10–15] For example, pulmonary artery ECs (PAECs) from PAH patients and animal models exhibit increased glycolytic activity and decreased mitochondrial OXPHOS activity implicating the Warburg effect, which is often accompanied by perivascular infiltration of inflammatory cells in PAH lungs and elevated levels of cytokines/chemokines

in the circulation.[12,16–18] Yet, the key determinants of molecular cross talk between inflammation and cellular metabolism and its regulatory features remain poorly defined. Thus, in this study, we investigated the interrelationships between inflammation and cellular metabolism in human arterial ECs and in mouse mesenteric vessels, uniquely focusing on integrative molecular mechanisms underlying different immunometabolic phenotypes. Owing to the central role of ECs in inflammation, knowledge of these immunometabolic phenotypes will likely be broadly applicable to a wide range of cardiovascular pathobiologies and diseases.

METHODS

A detailed Methods section and the Major Resources Table are included in the Data Supplement. No experiment-wide/across-test multiple test correction was applied; only within-test corrections were made. The selected images and blots were those that most accurately represent the mean of each experimental group and are of high quality.

Data Availability

All data that support the findings of this study are presented in this article and its Data Supplement. Reagents will be made available upon reasonable request to the corresponding author.

RESULTS

Inflammatory Stimuli Enhance Glucose Metabolism in ECs

We first used metabolomic profiling to investigate the metabolic alterations in primary human PAECs treated with an inflammatory stimulus, TNFα (tumor necrosis factor alpha) or lipopolysaccharide (LPS), for 24 hours. We screened 137 metabolites, with results showing that TNFα treatment significantly altered the levels of 100 metabolites (>±1.2-fold; $P<0.05$), of which 83 were significantly elevated and 17 were significantly reduced (Figure 1A; Table I in the Data Supplement). In contrast to TNFα, LPS considerably changed the levels of 84 metabolites (>±1.2-fold; $P<0.05$), of which 77 were significantly increased, with only 7 significantly decreased (Figure 1B; Table I in the Data Supplement). These differentially changed metabolites were intermediates of glucose and fatty acid metabolism, amino acid metabolism, nucleotide and nucleic acid metabolism, and others (Figure 1A and 1B; Figure IA through ID in the Data Supplement; Table I in the Data Supplement), indicating that the proinflammatory mediators, TNFα and LPS, extensively reprogram cellular metabolism in ECs.

Metabolite Sets Enrichment Analysis demonstrated that the metabolite sets related to glucose metabolism were highly enriched in the top 20 pathways in inflamed PAECs (Tables II and III in the Data Supplement), highlighting the broad role of glucose metabolism in the cellular inflammatory response. Indeed, TNFα or LPS greatly increased the levels of metabolites of the pay-off phase of glycolysis, including pyruvate (PYR), lactate (LAC), glyceraldehyde 3-phosphate, 3-phosphoglycerate, or phosphoenolpyruvate, while only TNFα treatment diminished the levels of intermediates of the preparatory phase of glycolysis, such as G6P (glucose 6-phosphate), fructose 1,6-bisphosphate, and dihydroxyacetone phosphate (Figure 1C). TNFα or LPS also elevated the levels of the tricarboxylic acid (TCA) cycle metabolites, aconitate, citrate, 2-oxoglutarate, succinate, fumarate, or malate, as well as the pentose phosphate pathway (PPP) metabolites, R5P (ribose 5-phosphate) and Se7P (sedoheptulose 7-phosphate; Figure 1C). Of note, while cellular ATP levels were well-maintained, TNFα or LPS stimulation induced 2-fold to 3-fold increases in the levels of the ATP hydrolysis products, ADP and AMP, and, thereby, significantly decreased the ATP/ADP and ATP/AMP ratios (Figure ID in the Data Supplement). These metabolomic profiling results indicate that glucose metabolism enhanced in response to inflammatory stimuli.

In support of these findings, results from glucose uptake flux and microscopy assays showed that glucose uptake was enhanced by 1.4-fold to 2-fold in PAECs exposed to inflammatory stimuli, which correlated with an increase in the efflux rate of LAC—the glycolytic end-product (Figure 1D through 1F), suggesting that the increased demand for glucose was partially due to enhanced glycolytic activity. To test whether the other two major metabolic pathways of glucose, the PPP and mitochondrial OXPHOS, also contribute to the increased uptake of glucose, we measured [^{14}C]-CO_2 release from cells cultured with radiolabeled [^{14}C]-glucose since both pathways can generate CO_2 by glucose oxidation (Figure 1G). As shown in Figure 1H, [^{14}C]-CO_2 release from uniformly labeled [^{14}C]-glucose was elevated by over 1.5-fold in TNFα- or LPS-treated cells, suggesting glucose oxidation is enhanced in inflammation.

We further characterized glucose oxidation and compared it to glycolysis by directly tracing the fates of glucose using [U-^{13}C]-glucose (Figure 1I). We found that the inflammatory mediators, TNFα or LPS, increased the labeled fragments (M+3) of PYR and LAC by ≈10% with a concomitant decrease in their unlabeled pools (M+0; Figure 1J and 1K), while the isotopomer distribution patterns of other glycolytic intermediates (eg, glyceraldehyde 3-phosphate, dihydroxyacetone phosphate, and 3-phosphoglycerate) remained unchanged (Figure IE in the Data Supplement). Intriguingly, TNFα or LPS also significantly elevated the labeled pools (M+2, M+4, and M+5) of the TCA cycle intermediates, citrate and aconitate, and concomitantly decreased the unlabeled M+0 or M+1 fragments of these two metabolites (Figure 1L and 1M; Figure IF in the Data Supplement). In addition, the labeling pools

ORIGINAL RESEARCH

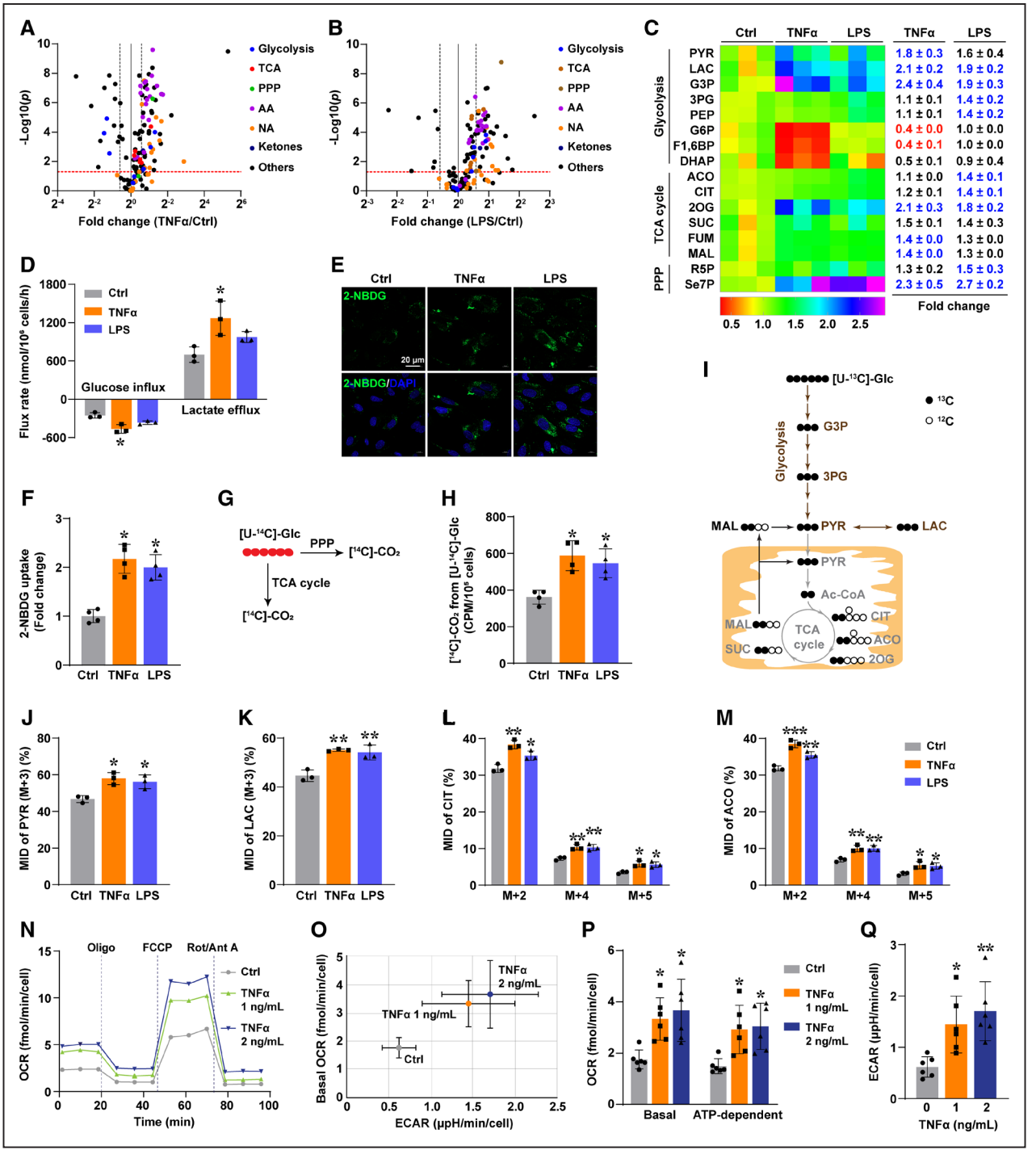

Figure 1. Inflammatory stimuli globally reprogram endothelial cell metabolism.
Confluent pulmonary artery endothelial cells (PAECs) were stimulated with TNFα (tumor necrosis factor alpha; 1 ng/mL) or lipopolysaccharide (LPS; 50 ng/mL) for 24 h. **A** and **B**, Volcano plots from metabolomic profiling using LC-MS show the fold changes of 137 metabolites in TNFα (**A**) or LPS (**B**) stimulated cells; n=3. **C**, Heat map and the fold changes of intermediate metabolites of glycolysis, the tricarboxylic acid (TCA) cycle, and the pentose phosphate pathway (PPP) relative to control cells; n=3. Significantly increased or decreased metabolites were indicated by blue or red, respectively ($P<0.05$ using the Kruskal-Wallis test followed by Dunn test). **D**, The flux rates of glucose uptake and lactate secretion; n=3. **E** and **F**, Representative images of 2-NBDG uptake (**E**) and corresponding quantitation (**F**) showing TNFα or LPS enhances glucose uptake in PAECs. Scale, 20 μm; n=4. **G** and **H**, [^{14}C]-CO_2 release from [U-^{14}C]-glucose (Glc) labeled cells; n=4. **I**, Schematic diagram showing the primary labeling patterns of [U-^{13}C]-Glc in glycolysis and the TCA cycle. **J**–**M**, The labeled fraction(s) of pyruvate (PYR; M+3; **J**), lactate (LAC; M+3; **K**), citrate (CIT; M+2, M+4, and M+5; **L**), and aconitate (ACO) (M+2, M+4, and M+5; **M**) using [U-^{13}C]-Glc as a tracer; n=3. **N**, Representative oxygen consumption rate (OCR) plot from a Seahorse mitochondrial stress assay. **O**, Energetics map showing basal OCR and extracellular acidification rate (ECAR) in TNFα-stimulated PAECs; n=6. **P** and **Q**, Quantitation of basal and ATP-dependent OCR (**P**), as well as glycolytic ECAR (**Q**) from the Seahorse assay; n=6. Data presented as mean±SD. *$P<0.05$, **$P<0.01$, and ***$P<0.001$ vs control by the Kruskal-Wallis test followed by Dunn test (**D**, **F**, **H**, **J**–**M**, **P**, and **Q**).

of other metabolites (eg, 2-oxoglutarate, succinate, and malate) in the TCA cycle were largely unaffected (Figure IF in the Data Supplement). Thus, these results support the conclusion that the fluxes of glucose into both glycolysis and the TCA cycle are enhanced in PAECs exposed to inflammatory stimuli.

These findings were further supported by measurements of oxygen consumption rate (OCR; indicative of mitochondrial OXPHOS) and extracellular acidification rate (ECAR; indicative of glycolysis) using the Seahorse XF analyzer. Results demonstrated that both basal and ATP-dependent OCR were increased from 1.5 to 1.8 fmol/min per cell in controls to 3 to 4 fmol/min per cell in TNFα-treated PAECs (Figure 1N through 1P). The same treatment also increased ECAR by 2-fold to 3-fold (Figure 1O and 1Q). Since glycolytic LAC, respiratory CO_2 hydrolysis, and ATP hydrolysis could lead to the increase in ECAR with their relative contribution depending upon cell type,[19,20] we further validated these findings by measurement of LAC secretion. As shown in Figure IG in the Data Supplement, TNFα stimulation elevated extracellular LAC levels by ≈2-fold, which correlated with the 2-fold to 3-fold increase in ECAR, implying that LAC is the primary source for the TNFα-induced increase in ECAR in PAECs. Of note, LPS challenge at high dose (50 ng/mL) enhanced basal and ATP-dependent OCR by 1.2-fold and ECAR by 2.1-fold; while low-dose LPS (10 ng/mL) increased ECAR by 1.7-fold with no change in OCR (Figure IH in the Data Supplement).

Since PAECs reside in a relatively low oxygen environment under physiological conditions and ECs are heterogeneous with specialized metabolic and functional responses based on the needs and niche of their resident tissues whose perfusion they govern,[1,21,22] we next investigated whether these metabolic alterations hold in inflamed human aortic ECs (AoECs)—a cell type living in an oxygen-rich niche under normal circumstances. Similarly, energetics mapping showed that the increases in OCR and ECAR were also observed in TNFα- or LPS-stimulated AoECs (Figure II and IJ in the Data Supplement). Therefore, these results reveal that inflammatory stimuli enhance both glycolysis and mitochondrial respiration in human pulmonary and systemic arterial ECs, irrespective of their origins or local oxygen tensions.

Taken together, results in Figure 1 indicate that the inflammatory mediators, TNFα and LPS, activate all 3 central glucose metabolic pathways in human arterial ECs. Activation of the PPP is required for the biosynthesis of nucleic acids (NAs), nucleotides, and cellular reducing equivalents, NADPH and glutathione (GSH), to sustain cell proliferation and survival, as well as for cellular redox homeostasis, while enhancements of both mitochondrial OXPHOS and more prominently glycolysis are essential for the replenishment and maintenance of the cellular ATP pool to accommodate increased ATP utilization in inflammatory states.

Inflammatory Mediators Modulate Gene Expression in Glucose Metabolism

Next, we performed RNA sequencing (RNA-seq) transcriptomic analysis to identify the potential molecular mediators of metabolic reprogramming in TNFα-treated PAECs. Principal component analysis showed TNFα-treated cells closely clustered and were clearly distinct from unstimulated cells (Figure IIA in the Data Supplement). Specifically, TNFα significantly upregulated 1820 genes (>1.5-fold; adjusted $P<0.05$) and suppressed 1609 genes (<0.7-fold; adjusted $P<0.05$; Figure IIB and IIC in the Data Supplement; Table IV in the Data Supplement). Inflammatory response-related genes/pathways were highly enriched in the top 10 gene ontology terms and KEGG pathways (Figure IID and IIE in the Data Supplement).

To understand the changes of metabolic genes, we next characterized a subset of 395 glucose metabolism–related genes based upon a published list of 1629 mammalian metabolic enzymes[23] and their protein functions using the UniProtKB database (Table IV in the Data Supplement). Among this subset, 69 and 75 genes were significantly stimulated or repressed (>±1.2-fold; adjusted $P<0.01$), respectively, of which *CYB5R2* was the most significantly upregulated (15-fold) and *PDK4* (*PYR dehydrogenase kinase 4*) was the most significantly downregulated (99.6%; Figure 2A through 2D; Table IV in the Data Supplement). Consistent with the enhanced glycolytic activity (Figure 1), the glycolytic genes *ALDOC*, *PFKFB3* (*6-phosphofructo-2-kinase/fructose 2,6-bisphosphatase 3*), *PFKFB4, PGMA1*, *SLC16A4* (aka *MCT5*), *SLC16A9* (ie, *MCT9*), and *SLC2A6* (ie, *GLUT6*) were upregulated by over 1.5-fold (Figure 2B and 2C). Furthermore, we also observed significant induction of mitochondrial respiratory complex genes *NDUFA9* and *COX17* (Figure 2B and 2C), which was accompanied by marked repression of these transcripts encoding proteins with inhibitory effects on mitochondrial respiratory activity, such as *PDK2*, *PDK4*, and *SLC25A27* (ie, *UCP4*; Figure 2B and 2D). These gene expression profiles are consistent with the enhanced activity of mitochondrial OXPHOS (Figure 1).

To validate these transcriptomic findings, we examined the mRNA expression of 14 key glucose metabolic genes. Consistent with RNA-seq findings, heat map and quantitation from quantitative RT-PCR (real time polymerase chain reaction) assays showed that TNFα upregulated glycolytic genes *GLUT4*, *PFKFB3*, and *PKM2* (*PYR kinase M2*) mRNA by 1.3-6-fold and that the same treatment repressed *PDK4* mRNA by over 90% and *PDK1* mRNA by <20% in PAECs (Figure 2E and 2F) and AoECs (Figure 2I and 2J). Interestingly, these gene expression changes were also observed in LPS-treated ECs but to a lesser extent relative to TNFα (Figure 2G and 2K). Concomitant immunoblotting results

ORIGINAL RESEARCH

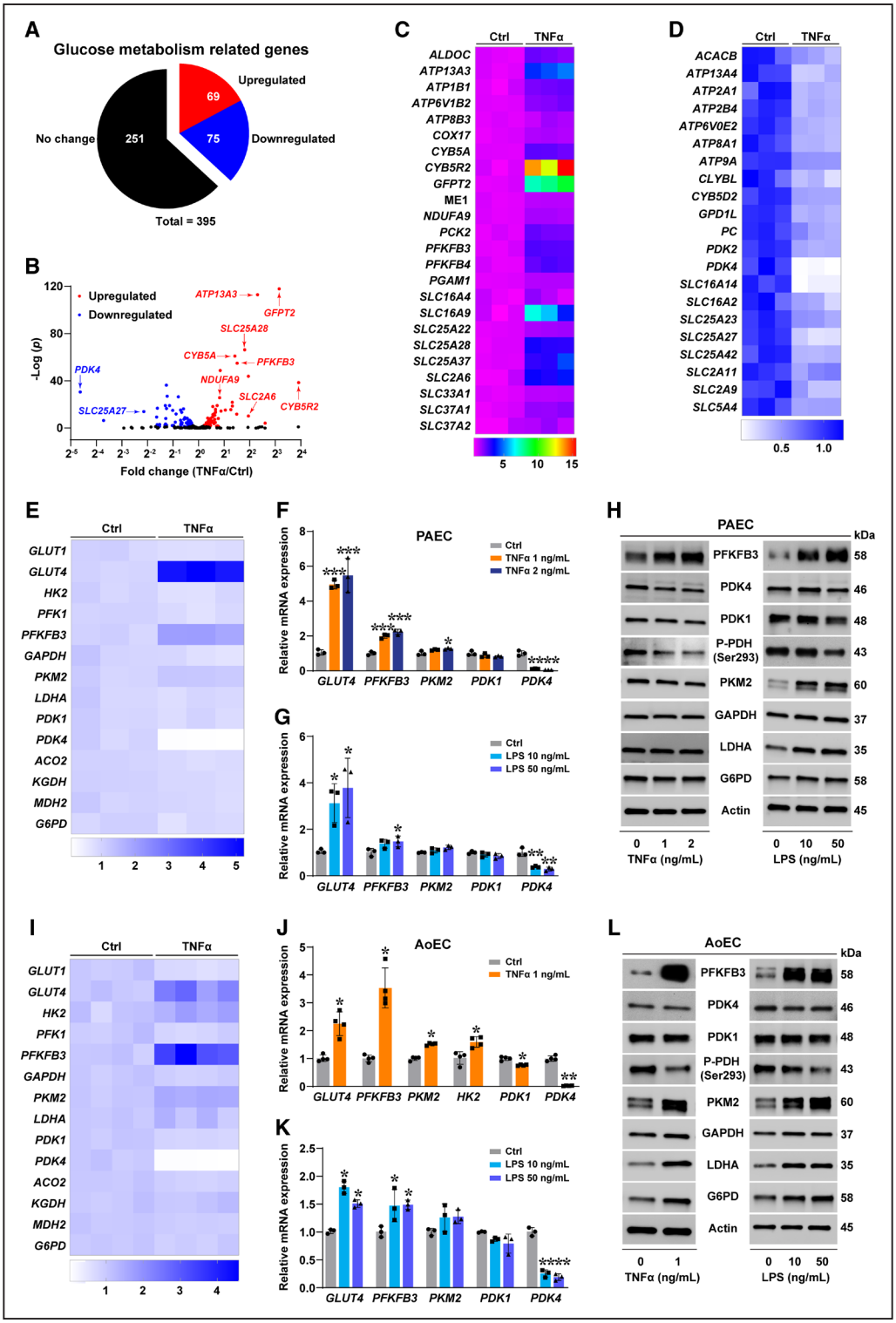

Figure 2. Inflammatory stimuli modulate metabolic gene expression.

A and **B**, Pie graph (**A**) and volcano plot (**B**) from RNA sequencing (RNA-seq) showing the expression profile of glucose metabolism–related genes in TNFα (tumor necrosis factor alpha)-stimulated pulmonary artery endothelial cells (PAECs), with upregulated genes (>1.2-fold) and downregulated genes (<0.8-fold), and adjusted $P<0.01$ by the Benjamini-Hochberg test; n=3. **C** and **D**, The upregulated genes (>1.5-fold) and downregulated genes (<0.5-fold) from RNA-seq analysis. Color scales represent fold changes relative to control cells; n=3. **E**, **F**, **I**, and **J**, Heat maps (**E** and **I**) and quantitative results (**F** and **J**) show mRNA expression of metabolic genes in PAECs (**E** and **F**; n=3) and aortic endothelial cell (AoECs; **I** and **J**, n=4) stimulated by TNFα for 24 h. Color scales in heat maps represent fold changes relative to control cells. **G** and **K**, mRNA expression of metabolic genes in PAECs (**G**) or AoECs (**K**) stimulated by lipopolysaccharide (LPS) for 24 h; n=3. **H** and **L**, The protein levels of select metabolic genes in TNFα- or LPS-challenged PAECs (**H**) or AoECs (**L**); n=3. Data presented as mean±SD. *$P<0.05$, **$P<0.01$, ***$P<0.001$, ****$P<0.0001$ vs control by the Kruskal-Wallis test followed by Dunn test (**F**, **G**, and **K**) or the Mann-Whitney *U* test (**J**).

revealed that TNFα and LPS enhanced PFKFB3 protein expression by ≈2-fold and 5-fold to 6-fold in PAECs, respectively (Figure 2H). The upregulation of PFKFB3 protein appeared to be greater in AoECs than PAECs (Figure 2L). In contrast to the 60% to 90% suppression of *PDK4* mRNA, we observed modest decreases in the protein levels of PDK4 and its isoform PDK1 by TNFα or LPS in both types of ECs (Figure 2H and 2L). These discordant changes in the magnitude of *PDK4* mRNA and protein were also reported in cardiomyocytes of PAH rats and in LPS-treated mouse C2C12 myoblasts.[24,25] Nevertheless, this modest reduction in PDK isoforms correlated with a marked decrease in the phosphorylation of their substrate PYR dehydrogenase (P-PDH; Figure 2H and 2L). Of note, G6PD (glucose 6-phosphate dehydrogenase; the rate-limiting enzyme of the PPP) activity was significantly elevated by TNFα or LPS treatment with a greater increase in LPS-treated PAECs (Figure IIF in the Data Supplement), which correlated with a higher level of G6PD protein by LPS than TNFα (Figure 2H), although its mRNA expression was not affected (Figure 2E and 2I; Figure IIG through IIJ in the Data Supplement).

It is noteworthy that these two inflammatory mediators differentially modulate metabolic gene expression within the same cell type and between different cell types. TNFα selectively stimulated *HK2* mRNA by 2-fold and repressed *GLUT1* and *ACO2* mRNA expression in AoECs (Figure 2I and 2J; Figure III in the Data Supplement). LPS markedly upregulated the protein levels of PKM2, LDHA, and G6PD in PAECs, whereas these changes were not observed with TNFα treatment (Figure 2H). By contrast, both TNFα and LPS significantly enhanced the expression levels of these proteins in AoECs (Figure 2L). Thus, these results identify both common and distinct gene expression patterns induced by 2 different inflammatory stimuli in 2 types of human arterial ECs.

The enzyme PFKFB3 catalyzes the conversion of F6P into F2,6BP, which is the most potent allosteric activator of PFK1 (phosphofructokinase 1)—the rate-limiting enzyme of glycolysis.[26] The upregulation of PFKFB3 and other glycolytic enzymes is consistent with the enhanced glycolytic activity in inflamed arterial ECs (Figures 1 and 2). PDH governs the fate of glucose-derived PYR in the TCA cycle, and, importantly, its enzymatic activity is controlled by PDK-mediated phosphorylation and inactivation.[27] The TNFα- or LPS-induced reductions in PDK4 expression and P-PDH protein levels lowered the threshold for PYR entry into the TCA cycle, leading to increased TCA cycle activity and mitochondrial respiration in ECs (Figures 1 and 2). In addition, since G6PD is the rate-limiting enzyme of the PPP, the elevations of G6PD protein levels and activity help explain the enhancement of the PPP (Figures 1 and 2).

Since PDK4, G6PD, and PFKFB3 are key enzymes in glucose metabolism and, importantly, changes in the expression and activity of these enzymes were robustly and commonly found in inflamed arterial ECs, we next sought to investigate comparatively the immunometabolic roles of these key regulatory proteins.

Restoration of PDK4 Function Inhibits Mitochondrial Respiration and Potentiates Inflammation

We first delineated the immunometabolic role of PDK4 by overexpressing it in PAECs followed by inflammatory stimulus challenge. Overexpressing *PDK4* was successful as functionally evidenced by significant increases in its mRNA and the phosphorylation of PDH protein (P-PDH) in unstimulated cells, and, importantly, by significant recovery of the reduced *PDK4* mRNA and P-PDH levels in TNFα- or LPS-stimulated cells (Figure 3A, 3F, and 3G; Figure IIIA in the Data Supplement). We next investigated whether and how *PDK4* overexpression influences metabolic alterations in the setting of inflammation. Results from the Seahorse assay showed that overexpression of *PDK4* greatly mitigated the increases in basal, ATP-dependent, and maximal OCR in PAECs challenged with inflammatory stimuli, although it did not significantly influence the elevated ECAR, consistent with the comparable and robust upregulation of *PFKFB3* mRNA in these cells (Figure 3B through 3E; Figure IIIB through IIIG in the Data Supplement; see below). Likewise, blockade of the transport of PYR into mitochondria by UK5099—a pharmacological inhibitor of the mitochondrial PYR carrier[28]—completely normalized LPS-induced elevations in OCR but without significant effects on ECAR (Figure IIII through IIIK in the Data Supplement). Thus, these observations indicate that the enhancement of mitochondrial OXPHOS in the setting of inflammation is mediated, in part, by repression of *PDK4* expression and, consequently, increases in PDH complex activity and PYR oxidation in PAECs.

Enhanced mitochondrial respiration has been shown to support the anti-inflammatory phenotype of IL-4–stimulated macrophages.[29] As there is a lack of understanding as to how enhanced mitochondrial oxidation of glucose regulates inflammatory responses in human arterial ECs, we addressed this problem using *PDK4*-overexpressing PAECs. Results from quantitative RT-PCR and immunoblotting assays revealed that overexpression of *PDK4* strongly potentiated TNFα- or LPS-induced mRNA and protein upregulation of the proinflammatory adhesion molecules, VCAM1 (vascular cell adhesion molecule 1), ICAM1 (intercellular adhesion molecule 1), or CCL2 (C-C motif chemokine ligand 2; Figure 3F through 3I; Figure IIIH in the Data Supplement), which was accompanied by a potentiation of monocyte adhesion to inflamed PAECs with *PDK4* overexpression (Figure 3J). Furthermore, inhibition of mitochondrial respiration using UK5099 or complex III inhibitor antimycin A markedly exacerbated

ORIGINAL RESEARCH

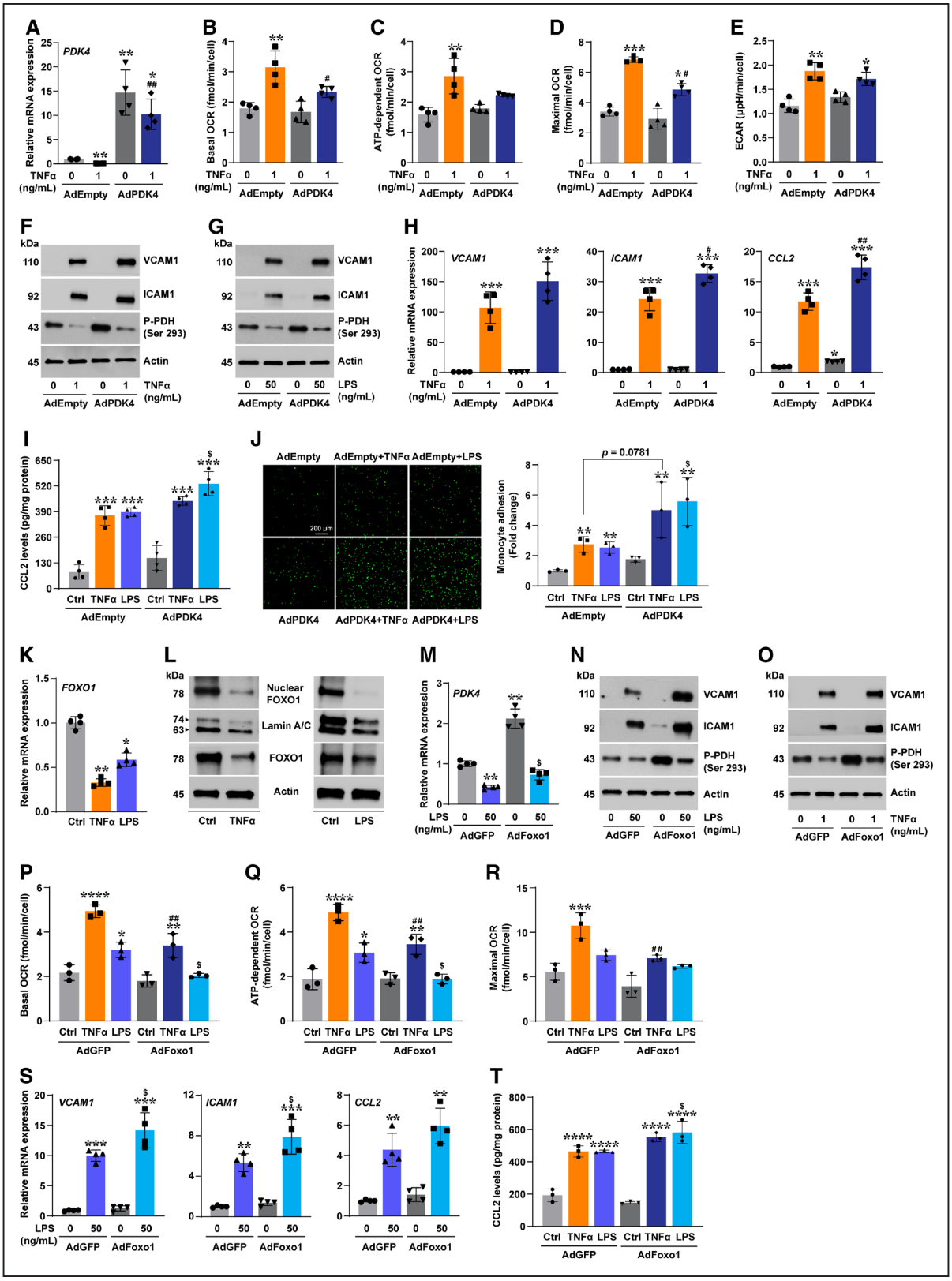

Figure 3. Restoration of the FOXO1 (forkhead box O1)-PDK4 (pyruvate dehydrogenase kinase 4) pathway suppresses mitochondrial respiration but worsens inflammation.

A, *PDK4* mRNA levels in adenoviral *PDK4* vector (AdPDK4; 20 MOI) or empty vector (AdEmpty) transfected pulmonary artery endothelial cells (PAECs) with or without TNFα (tumor necrosis factor alpha) stimulation for 24 h; n=4. **B**–**E**, Basal oxygen consumption rate (OCR; **B**), ATP-dependent OCR (**C**), maximal OCR (**D**), and extracellular acidification rate (ECAR; **E**) from a Seahorse mitochondrial stress test; n=4. **F** and **G**, Protein levels of ICAM1 (intercellular adhesion molecule 1), VCAM1 (vascular cell adhesion molecule 1), (*Continued*)

the induction of ICAM1 or VCAM1 expression by TNFα or LPS (Figure IIIL through IIIN in the Data Supplement). Overall, these findings indicate that overexpression of *PDK4* abrogates the enhancement of mitochondrial respiration and heightens inflammatory responses, indicating that the metabolic enhancement of mitochondrial respiration suppresses inflammatory response in human arterial ECs.

To investigate the molecular mechanism(s) mediating *PDK4* repression induced by inflammatory stimuli, we focused on the transcription factor *FOXO1* (*forkhead box O1*) since FOXO1 has been shown to upregulate *PDK4* transcription,[30] and our RNA-seq results showed a 50% reduction of *FOXO1* mRNA in TNFα-treated PAECs (Table IV in the Data Supplement). Importantly, the role of the FOXO1-PDK4 axis in modulating inflammation in ECs remains unexplored. Consistent with RNA-seq analysis, quantitative RT-PCR and immunoblotting assays revealed that TNFα or LPS treatment significantly suppressed FOXO1 expression and nuclear translocation (Figure 3K and 3L), indicating that the transcriptional activity of FOXO1 is inhibited. To test the immunometabolic role of FOXO1-PDK4 signaling, we overexpressed (mouse) *Foxo1* in human PAECs. The overexpressed Foxo1 protein was confirmed to be successful as functionally demonstrated by a significant (over 2-fold) upregulation of *PDK4* mRNA, as well as P-PDH protein levels (Figure 3M through 3O; Figure IIIO in the Data Supplement). Similar to *PDK4* overexpression, overexpression of *Foxo1* also attenuated TNFα- or LPS-induced increases in OCR with no impact on the elevated ECAR (Figure 3P through 3R; Figure IIIP in the Data Supplement). The mitigation of increased OCR correlated with significant restoration of reduced *PDK4* mRNA and P-PDH protein levels in *Foxo1* overexpressing and inflamed PAECs (Figure 3M through 3O). Importantly, normalization of this metabolic alteration potentiated inflammatory responses as the induction of inflammatory adhesion molecules, ICAM1, VCAM1, and CCL2 mRNA or protein, was significantly augmented in *Foxo1* overexpressing cells treated with TNFα or LPS (Figure 3N, 3O, 3S, and 3T). Taken together, these findings reveal that inhibition of the FOXO1-PDK4 signaling pathway by inflammatory stimuli leads to the enhancement of mitochondrial oxidation of glucose, which has anti-inflammatory consequences in human arterial ECs.

Inhibition of G6PD Enhances Glycolysis and Worsens Inflammation

Next, we elucidated the immunometabolic role of G6PD in ECs. Silencing *G6PD* strongly upregulated the mRNA or protein expression of VCAM1, ICAM1, and CCL2 in unstimulated PAECs and also significantly exacerbated LPS-induced upregulation of these molecules (Figure 4A, 4B, and 4F). Similar effects were also observed, to a lesser extent, in TNFα-treated cells (Figure 4C and 4F; Figure IVA in the Data Supplement). Likewise, inhibition of G6PD activity with DHEA—a pharmacological inhibitor of G6PD[31]—augmented the elevated levels of ICAM1 and VCAM1 proteins in TNFα- or LPS-exposed cells (Figure 4D and 4E). Functionally, the augmented expression of these adhesion molecules led to greater monocyte adhesion to PAECs with *G6PD* silencing under basal and inflammatory conditions (Figure 4G). These lines of evidence clearly support the conclusion that blockade of the PPP by G6PD inactivation worsens the inflammatory response in PAECs, implying that activation of the PPP also has anti-inflammatory consequences.

Since the PPP is required for maintenance of redox homeostasis through recycling redox equivalents, NADPH and GSH,[32,33] and oxidative stress is commonly seen in inflammatory states, we speculated that G6PD inhibition perturbs cellular redox balance leading to exacerbated inflammation. As anticipated, TNFα or LPS induced oxidative stress in PAECs as evidenced by a catalase-inhibitable increase in H_2DCF oxidation, an upregulation of NOX4 (NADPH oxidase 4) protein (but not its mRNA), a decrease in cellular NADPH levels, and a modestly elevated $NADP^+$/NADPH ratio (Figure IVA through IVF in the Data Supplement). Surprisingly, inhibition of *G6PD* failed to augment such oxidative stress, which correlated with an exacerbated repression of *NOX4* mRNA and a partial normalization of the upregulated NOX4 protein despite greater LPS-induced reductions in cellular NADP(H) levels and an increase in the $NADP^+$/NADPH ratio (Figure IVA through IVF in the Data Supplement). This effect may be a reflection of both decreased NOX4-dependent utilization of and decreased

Figure 3 Continued. and P-PDH in PAECs with 24 h of TNFα (**F**) or lipopolysaccharide (LPS; **G**) stimulation; n=3. **H**, mRNA expression of inflammatory adhesion molecules in TNFα-stimulated cells; n=4. **I**, CCL2 (C-C motif chemokine ligand 2) levels in PAECs transfected with AdEmpty or AdPDK4; n=4. **J**, Representative images (**left**; scale, 200 μm) and quantitation (**right**) showing monocyte adhesion to the lawn of PAECs; n=3. **K** and **L**, *FOXO1* mRNA (**K**; n=4) and protein (**L**; n=3) expression in PAECs challenged with TNFα or LPS for 24 h. **M**, *PDK4* mRNA expression in PAECs transfected with adenoviral vector of mouse *Foxo1* (AdFoxo1; 80 MOI) or GFP control (AdGFP) followed by 24-h stimulation of LPS; n=4. **N** and **O**, Protein levels of ICAM1, VCAM1, and P-PDH in *Foxo1* overexpressed cells with the stimulation of LPS (**N**) or TNFα (**O**) for 24 h; n=3. **P**–**R**, The Seahorse mitochondrial stress test shows basal OCR (**P**), ATP-dependent OCR (**Q**), and maximal OCR (**R**) in PAECs transfected with AdFoxo1 or AdGFP followed by 24-h stimulation of TNFα or LPS; n=3. **S**, mRNA expression of inflammatory marker genes in *Foxo1* overexpressed and LPS-stimulated cells; n=4. **T**, CCL2 levels in PAECs transfected with AdGFP or AdFoxo1 followed by inflammatory stimuli for 24 h; n=3. Data presented as mean±SD. **P*<0.05, ***P*<0.01, ****P*<0.001, *****P*<0.0001 vs control by the Kruskal-Wallis test followed by Dunn test (**A**–**E**, **H**–**K**, **M**, and **P**–**T**); #*P*<0.05 and ##*P*<0.01 vs AdEmpty- or AdGFP-transfected and TNFα-stimulated cells by Dunn test (**A**, **B**, **D**, **H**, and **P**–**R**); $*P*<0.05 vs AdEmpty- or AdGFP-transfected and LPS-stimulated cells by Dunn test (**I**, **J**, **M**, **P**, **Q**, **S**, and **T**).

ORIGINAL RESEARCH

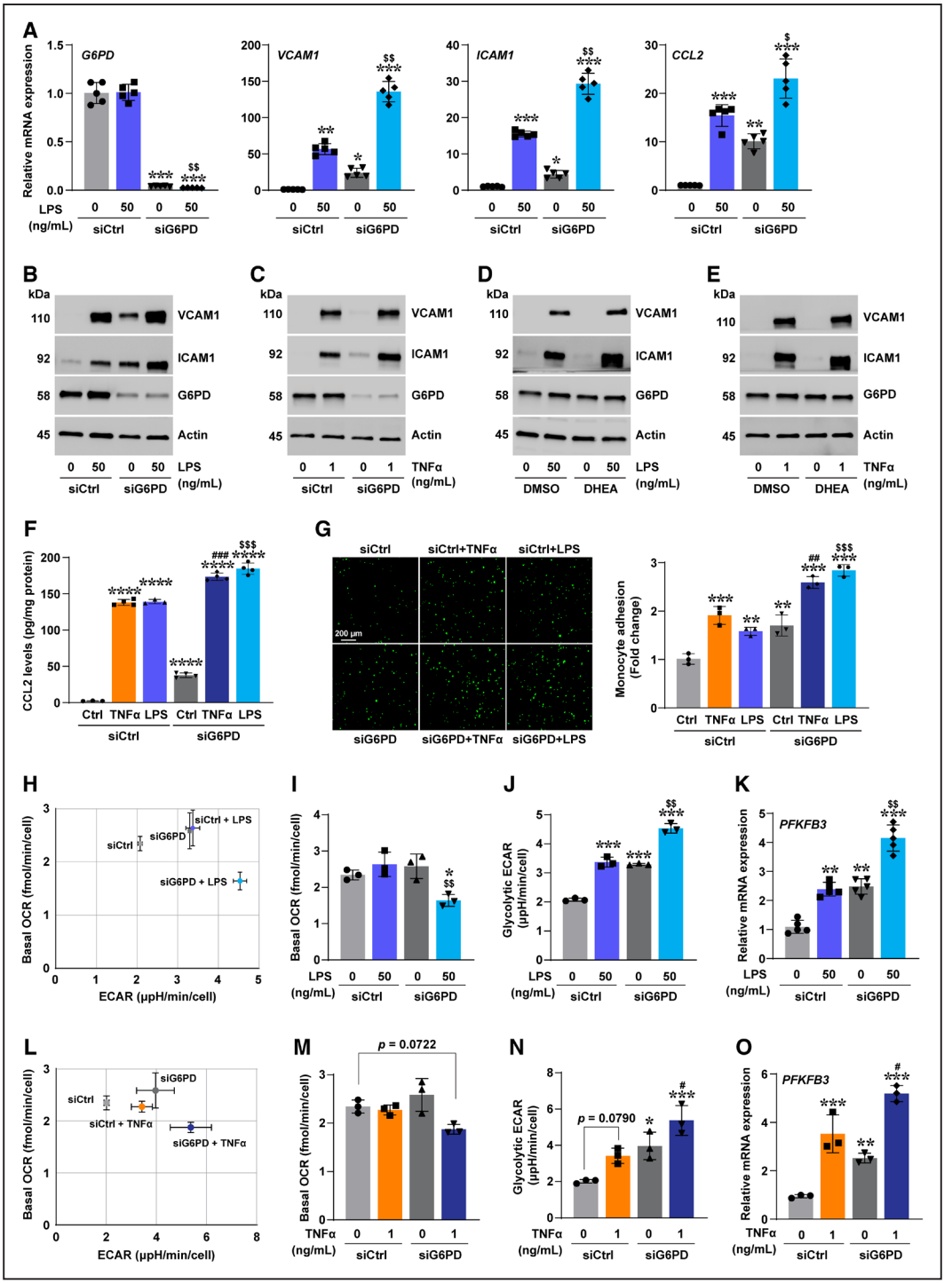

Figure 4. Inhibition of G6PD (glucose 6-phosphate dehydrogenase) promotes a metabolic shift to glycolysis and inflammation. **A**, mRNA expression of *G6PD* and adhesion molecules in human *G6PD* siRNA (siG6PD) or control siRNA (siCtrl) transfected pulmonary artery endothelial cells (PAECs) with or without lipopolysaccharide (LPS) stimulation for 8 h; n=5. **B**–**E**, Protein levels of G6PD, ICAM1 (intercellular adhesion molecule 1), and VCAM1 (vascular cell adhesion molecule 1) in PAECs with *G6PD* silencing by siRNA (**B** and **C**) or inactivation by the enzymatic inhibitor DHEA (50 μM; **D** and **E**) under LPS (**B** and **D**) or TNFα (tumor necrosis factor alpha; **C** and **E**) stimulation for 8 h; n=3. **F**, CCL2 (C-C motif chemokine ligand 2) levels in PAECs with *G6PD* silencing and 8 h of inflammatory stimuli challenge; n=3 to 4. **G**, Representative images (**left**; scale, 200 μm) and corresponding quantitation (**right**) show the adhesion of monocytes to the lawn of PAECs; n=3. **H** and **L**, Energetics maps showing basal oxygen consumption rate (OCR) and extracellular acidification rate (ECAR) in LPS- (**H**) or TNFα- (**L**) treated and *G6PD* silenced PAECs for 8 h; n=3. **I**, **J**, **M**, and **N**, Seahorse mitochondrial stress assays showing basal OCR (**I** and **M**) and glycolytic ECAR (**J** and **N**) after 8 h of LPS (**I** and **J**) or TNFα (**M** and **N**) stimulation; n=3. **K** and **O**, *PFKFB3* mRNA expression in LPS- (**K**; n=5) or TNFα- (**O**; n=3) stimulated PAECs for 8 h. Data presented as mean±SD. **P*<0.05, ***P*<0.01, ****P*<0.001, *****P*<0.0001 vs control by the Kruskal-Wallis test followed by Dunn test (**A**, **F**, **G**, **I**–**K**, **N**, and **O**); #*P*<0.05, ##*P*<0.01, ###*P*<0.001 vs siCtrl-transfected and TNFα-treated cells by Dunn test (**F**, **G**, **N**, and **O**); $*P*<0.05, $$*P*<0.01, $$$*P*<0.001 vs siCtrl-transfected and LPS-stimulated cells by Dunn test (**A**, **F**, **G**, **I**, and **J**).

G6PD-dependent synthesis of its cosubstrate NADPH (Figure IVF in the Data Supplement). In addition, and as anticipated, G6PD inactivation by DHEA lowered cellular total GSH (GSH+GSSG [oxidized GSH]) and reduced GSH levels; however, it failed to potentiate LPS-induced changes in cellular GSH and GSSG levels or the GSSG/GSH ratio (Figure IVG in the Data Supplement). Thus, these findings indicate that G6PD inhibition–induced potentiation of inflammation may be accompanied by an increase in oxidative stress.

We next examined the effect of blockade of the PPP on glycolysis and augmentation of the inflammatory response. Results from Seahorse assays showed that LPS or TNFα treatment for 8 hours increased ECAR by over 62% but did not influence basal OCR in PAECs (Figure 4H through 4J and 4L through 4N), indicating a metabolic switch toward glycolysis. This metabolic shift was also observed in G6PD-silenced and unstimulated cells (Figure 4H through 4J and 4L through 4N). Strikingly, silencing of G6PD greatly attenuated basal OCR but strongly potentiated the increase in ECAR in cells challenged by either stimulus (Figure 4H through 4J and 4L through 4N), clearly indicating that blockade of the PPP by *G6PD* knockdown reprograms EC metabolism to glycolysis under both basal and inflammatory conditions. Consistent with this metabolic shift, we also found that *PFKFB3* mRNA expression was significantly upregulated by *G6PD* knockdown or inflammatory stimulus and that this upregulation was even further potentiated in inflamed cells with *G6PD* silencing (Figure 4K and 4O). Taken together, these results support the view that (1) the PPP supports an anti-inflammatory response in PAECs, (2) the metabolic switch to glycolysis strongly correlates with an augmented inflammatory response in G6PD-inhibited cells with or without inflammatory stimuli, and (3) PFKFB3 may be a crucial mediator of these immunometabolic effects.

PFKFB3 Mediates Inflammatory Stimuli-Induced Enhancement of Glycolysis

To characterize further the role of PFKFB3 in regulating immunometabolism, we first examined whether PFKFB3 is the crucial driver for enhanced glycolysis in the setting of inflammation. We found that *PFKFB3* silencing alone significantly lowered glycolytic ECAR and simultaneously increased basal OCR in PAECs (Figure 5A through 5D; Figure VA and VB in the Data Supplement), indicating that *PFKFB3* silencing blocks glycolysis and switches cellular metabolism to mitochondrial respiration in the basal state. Notably, this is also true with inflammatory stimulation because *PFKFB3* silencing markedly abrogated the TNFα-induced increase in glycolytic ECAR with a concomitant potentiation in the elevations of basal OCR at 6 and 24 hours (to a lesser extent; Figure 5A through 5D; Figure VA and VB in the Data Supplement). Consistent with the correction of the increased ECAR, *PFKFB3* knockdown greatly attenuated the increases in LAC secretion and [U-^{13}C]-Glc labeled fraction (M+3) of LAC and PYR in both unstimulated and inflamed PAECs (Figure 5E; Figure VC through VE in the Data Supplement). By contrast, when human *PFKFB3* was overexpressed in PAECs, in the presence of TNFα stimulation, the elevated levels of both *PFKFB3* mRNA and protein were further potentiated (Figure 5F and 5O), which correlated with significant enhancement of TNFα-induced increases in glycolytic ECAR, glycolytic capacity, and surprisingly basal OCR (Figure 5G through 5J).

Mechanistically, these effects on glycolytic activity were mainly mediated by PFKFB3 expression since TNFα- or LPS-induced changes of glycolytic proteins LDHA and PKM2, as well as G6PD protein, were not significantly influenced by *PFKFB3* manipulation (Figure VF through VJ in the Data Supplement). Moreover, *PFKFB3* knockdown or overexpression diminished the phosphorylation of PDH (P-PDH) in unstimulated cells and exacerbated such reduction in TNFα- or LPS-stimulated cells (Figure 5K, 5L, and 5O). Similar effects were also observed when PFKFB3 activity was inhibited using the pharmacological inhibitor 3-PO[34] or its derivative PFK15[35] (Figure 5M and 5N). These findings explain the increase in basal OCR in cells with *PFKFB3* modulation because a decrease in P-PDH levels enhances its activity and, thereby, increases the entry of PYR into the TCA cycle and mitochondrial OXPHOS to boost oxygen consumption. Overall, these observations indicate not only that PFKFB3 is the major enzyme controlling glycolysis, but also that blockade of glycolysis by PFKFB3 inactivation diverts glucose metabolism to mitochondrial respiration in PAECs under both unstimulated and inflammatory conditions.

PFKFB3-Mediated Enhancement of Glycolysis Promotes Inflammation

We next investigated how PFKFB3-mediated enhancement of glycolysis influences inflammation. Knockdown of *PFKFB3* clearly abrogated TNFα- or LPS-induced upregulation of inflammatory adhesion molecules in ECs, which was correlated with inhibition of the increased total p65 protein levels (Figure 5K, 5L, 5P, 5Q; Figure VK in the Data Supplement). Consequently, the TNFα- or LPS-induced increase in monocyte adhesion to PAECs was completely normalized by silencing *PFKFB3* (Figure 5R). Likewise, when PFKFB3 enzymatic activity was inhibited by the pharmacological inhibitors 3-PO or PFK15, the enhanced levels of VCAM1 and ICAM1 proteins were also markedly attenuated in inflamed PAECs; however, these changes weakly correlated with total p65 protein (Figure 5M and 5N). By contrast, in *PFKFB3* overexpressing PAECs, TNFα-induced upregulation of VCAM1, ICAM1, and CCL2 protein, but not total p65 protein, was

ORIGINAL RESEARCH

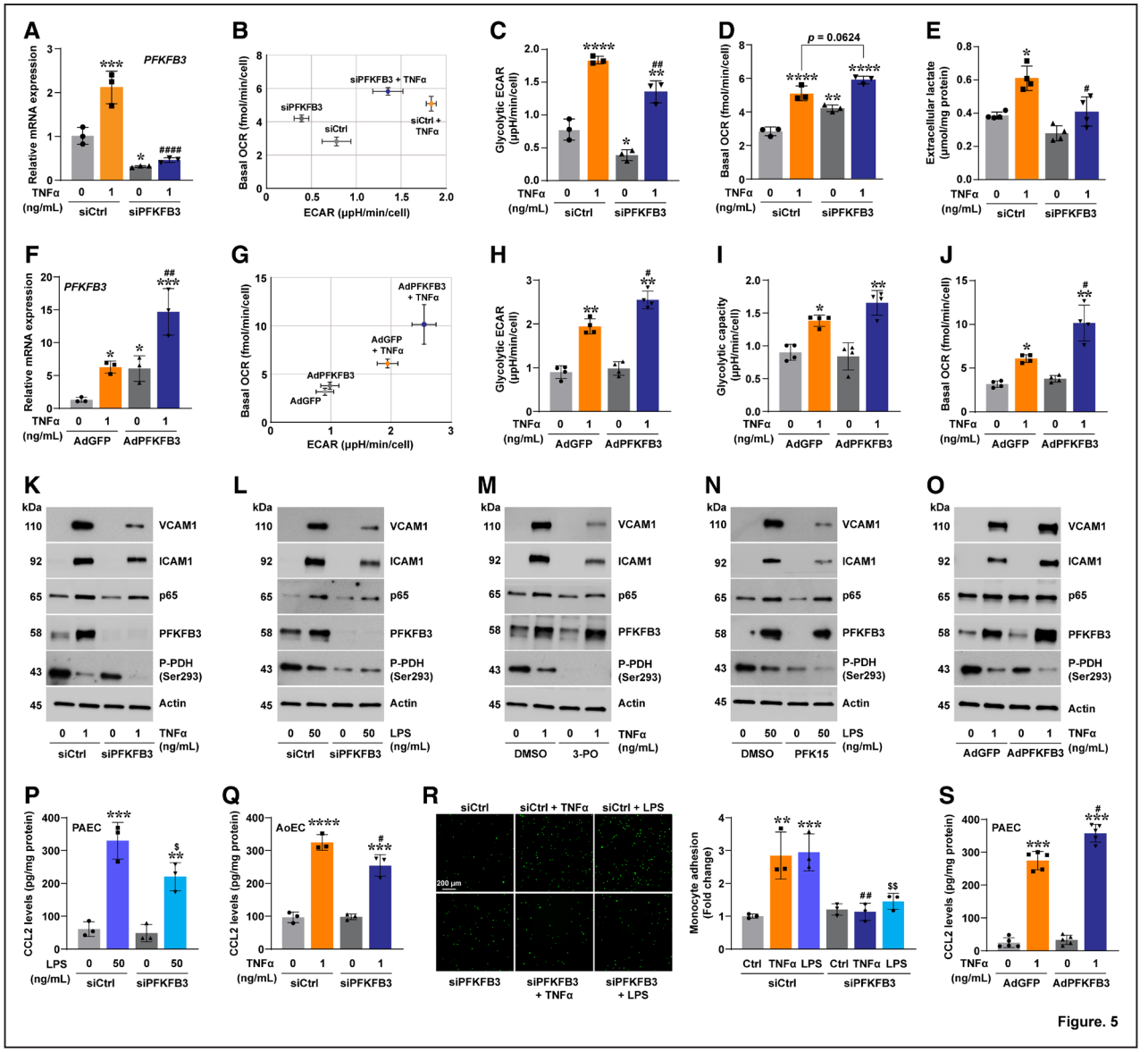

Figure 5. PFKFB3 (6-phosphofructo-2-kinase/fructose 2,6-bisphosphatase 3) is an essential immunometabolic regulator. **A** and **F**, *PFKFB3* mRNA expression in pulmonary artery endothelial cells (PAECs) with *PFKFB3* silencing by siRNA (siPFKFB3; **A**) or overexpression by adenoviral vector (AdPFKFB3; 60 MOI; **F**) followed by TNFα (tumor necrosis factor alpha) stimulation for 24 h; n=3. **B** and **G**, Energetics maps from a Seahorse glycolysis stress assay show basal oxygen consumption rate (OCR) and extracellular acidification rate (ECAR) in *PFKFB3* silenced (**B**; n=3) or overexpressed (**G**; n=4) PAECs with TNFα stimulation. **C** and **D**, Quantitation of glycolytic ECAR (**C**) and basal OCR (**D**) from the Seahorse assay; n=3. **E**, Extracellular lactate levels determined by a colorimetric assay in PAECs with TNFα stimulation for 24 h; n=4. **H**–**J**, Quantitation of glycolytic ECAR (**H**), glycolytic capacity (**I**), and basal OCR (**J**) from the Seahorse assay; n=4. **K**–**N**, Immunoblots showing the levels of inflammatory and metabolic proteins in PAECs with *PFKFB3* knockdown by siRNA (**K** and **L**) or inactivation by enzymatic inhibitors 3-PO (20 μM; **M**) or PFK15 (6 μM; **N**) in the presence or absence of TNFα (**K** and **M**) or lipopolysaccharide (LPS; **L** and **N**); n=3. **O**, Immunoblots showing the levels of inflammatory and metabolic proteins in PAECs with *PFKFB3* overexpression and TNFα stimulation for 6 h; n=3. **P** and **Q**, CCL2 (C-C motif chemokine ligand 2) levels in LPS-stimulated PAECs (**P**) and TNFα-stimulated aortic endothelial cells (**Q**); n=3. **R**, Monocyte adhesion to the lawn of PAECs (**left**; scale, 200 μm) and quantitative bar graph (**right**) in cells with *PFKFB3* silencing and inflammatory stimuli for 24 h; n=3. **S**, CCL2 levels in *PFKFB3* overexpressed and TNFα-treated PAECs; n=5. Data presented as mean±SD. **P*<0.05, ***P*<0.01, ****P*<0.001, *****P*<0.0001 vs control by the Kruskal-Wallis test followed by Dunn test (**A**, **C**–**F**, **H**–**J**, and **P**–**S**); #*P*<0.05, ##*P*<0.01, ####*P*<0.0001 vs siCtrl- or AdGFP–-transfected and TNFα-challenged cells by Dunn test (**A**, **C**, **E**, **F**, **H**, **J**, and **Q**–**S**); $*P*<0.05 and $$*P*<0.01 vs siCtrl-transfected and LPS-challenged cells by Dunn test (**P** and **R**).

potentiated by ≈1.5-fold (Figure 5O and 5S). Thus, results from loss/gain-of-function experiments with *PFKFB3* clearly suggest that PFKFB3 crucially mediates inflammatory response in ECs. These results, taken together with the metabolic findings described above, support the conclusion that PFKFB3 is a pivotal immunometabolic regulator and that the PFKFB3-mediated enhancement of glycolysis promotes inflammation.

This conclusion was further strengthened by results from the Seahorse assay showing that TNFα treatment

(2 ng/mL for 6 hours) increased ECAR 2-fold without affecting OCR (Figure VL and VM in the Data Supplement). Such selective enhancement of glycolysis correlated with the upregulated mRNA expression of *PFKFB3* and adhesion molecules (Figure VN in the Data Supplement). Moreover, as shown in Figure I in the Data Supplement, a low dose of LPS (10 ng/mL for 24 hours) enhanced ECAR but not OCR in PAECs (Figure VO and VP in the Data Supplement), which was accompanied by a 1.5-fold upregulation of *PFKFB3* mRNA and a 5-fold to 6-fold increase in *VCAM1*, *ICAM1*, and *CCL2* mRNA (Figure VQ in the Data Supplement).

Since the key glycolytic enzyme PKM2 was upregulated by inflammatory stimuli (Figure 2), we postulated that silencing *PKM2* could also inhibit the inflammatory response. Indeed, knockdown of *PKM2* considerably mitigated TNFα- or LPS-induced elevations of VCAM1, ICAM1, and p65 proteins in PAECs and did so in correlation with a normalization of PFKFB3 protein upregulation (Figure VR and VS in the Data Supplement). Of note, *PKM2* silencing alone also induced a compensatory elevation of PFKFB3 protein (Figure VR and VS in the Data Supplement). Thus, these observations further confirm that enhancement of glycolysis promotes the inflammatory response and does so via PFKFB3-mediated events.

Taken together, these data provide strong evidence in support of the hypothesis that PFKFB3 upregulation enhances glycolysis leading to promotion of inflammation in human arterial ECs.

NF-κB Pathway Transcriptionally Upregulates PFKFB3 Expression

To explore the underlying mechanism(s) by which inflammatory stimuli induce *PFKFB3* transcription, we focused on transcription factor NF-κB (nuclear factor-kappa B) since KEGG pathway analysis from RNA-seq showed that the NF-κB pathway was among the top 6 profoundly activated pathways in TNFα-stimulated cells (Figure IIE in the Data Supplement), and, importantly, bioinformatics analysis predicted 4 potential binding sites (S1–S4) in a 2-kb promoter region of the human *PFKFB3* gene (Figure 6A). Results from time sequence experiments revealed that TNFα promoted nuclear translocation of p65 protein after as brief as 10 minutes of stimulation leading to upregulation of *VCAM1* mRNA appearing after 30 minutes, and that inductions of *PFKFB3* mRNA and its protein were observed after 1 and 2 hours of TNFα treatment, respectively (Figure VIA and VIB in the Data Supplement). These results indicate that activation of the NF-κB pathway precedes PFKFB3 upregulation upon TNFα stimulation and raise the possibility that NF-κB regulates *PFKFB3* transcription.

Indeed, results from the ChIP (chromatin immunoprecipitation) assay showed that the binding of p65 protein to the 4 potential sites of human *PFKFB3* promoter region was highly enriched in TNFα-stimulated cells compared with untreated control cells, predominantly at the site nearest to the transcription start site (S1; Figure 6B). To validate further these findings, we blocked the NF-κB pathway using a pharmacological inhibitor PDTC.[36] PDTC pretreatment completely normalized the increased p65 nuclear translocation and the upregulated adhesion molecules in inflamed ECs, confirming its inhibitory efficacy on the NF-κB pathway (Figure VID through VIG in the Data Supplement). Notably, PDTC pretreatment significantly attenuated TNFα- or LPS-induced upregulation of the *PFKFB3* transcript and protein expression but unexpectedly induced a 2-fold increase in *PFKFB3* mRNA (Figure 6C; Figure VID through VIG in the Data Supplement). To circumvent this off-target effect, we inactivated NF-κB signaling by overexpression of a dominant-negative IκBα protein (IκBα[DN]).[37] As with PDTC, IκBα(DN) overexpression successfully abolished the increases in p65 nuclear translocation and protein levels of inflammatory markers in inflamed ECs (Figure 6E and 6F; Figure VIH and VII in the Data Supplement). Importantly, cells with IκBα(DN) overexpression were resistant to TNFα- or LPS-induced *PFKFB3* mRNA and protein upregulation compared with control cells (Figure 6D through 6F; Figure VIC, VIH, and VII in the Data Supplement). These data support *PFKFB3* as a newly identified transcriptional target of the NF-κB pathway.

Inactivation of NF-κB Signaling Suppresses Inflammation via Normalization of PFKFB3-Mediated Enhancement of Glycolysis

It is well-accepted that inactivation of NF-κB signaling inhibits inflammation by transcriptionally suppressing inflammatory molecules. However, it is unclear as to whether or not some aspect of basic cell metabolism could be a potential mechanism mediating this effect. Here, our evidence indicates that blockade of NF-κB pathway normalizes inflammation and PFKFB3 upregulation (Figure 6C through 6F; Figure VIC through VII in the Data Supplement) and that PFKFB3-mediated enhancement of glycolysis supports inflammation (Figure 5). Therefore, we hypothesized that inhibition of NF-κB signaling suppresses inflammation by blocking the PFKFB3-mediated stimulation of glycolysis.

To test this hypothesis, we evaluated cellular metabolic activity in ECs with IκBα(DN) protein overexpression. Results from the Seahorse assay showed that overexpression of IκBα(DN) significantly attenuated TNFα-induced elevation in ECAR in PAECs (Figure 6G and 6H) and AoECs (Figure VIJ and VIK in the Data Supplement), indicating an inhibition of glycolysis. This finding correlated with a concomitant alleviation of PFKFB3 upregulation in ECs with NF-κB signaling inactivation (Figure 6C through 6F; Figure VIC through VII

ORIGINAL RESEARCH

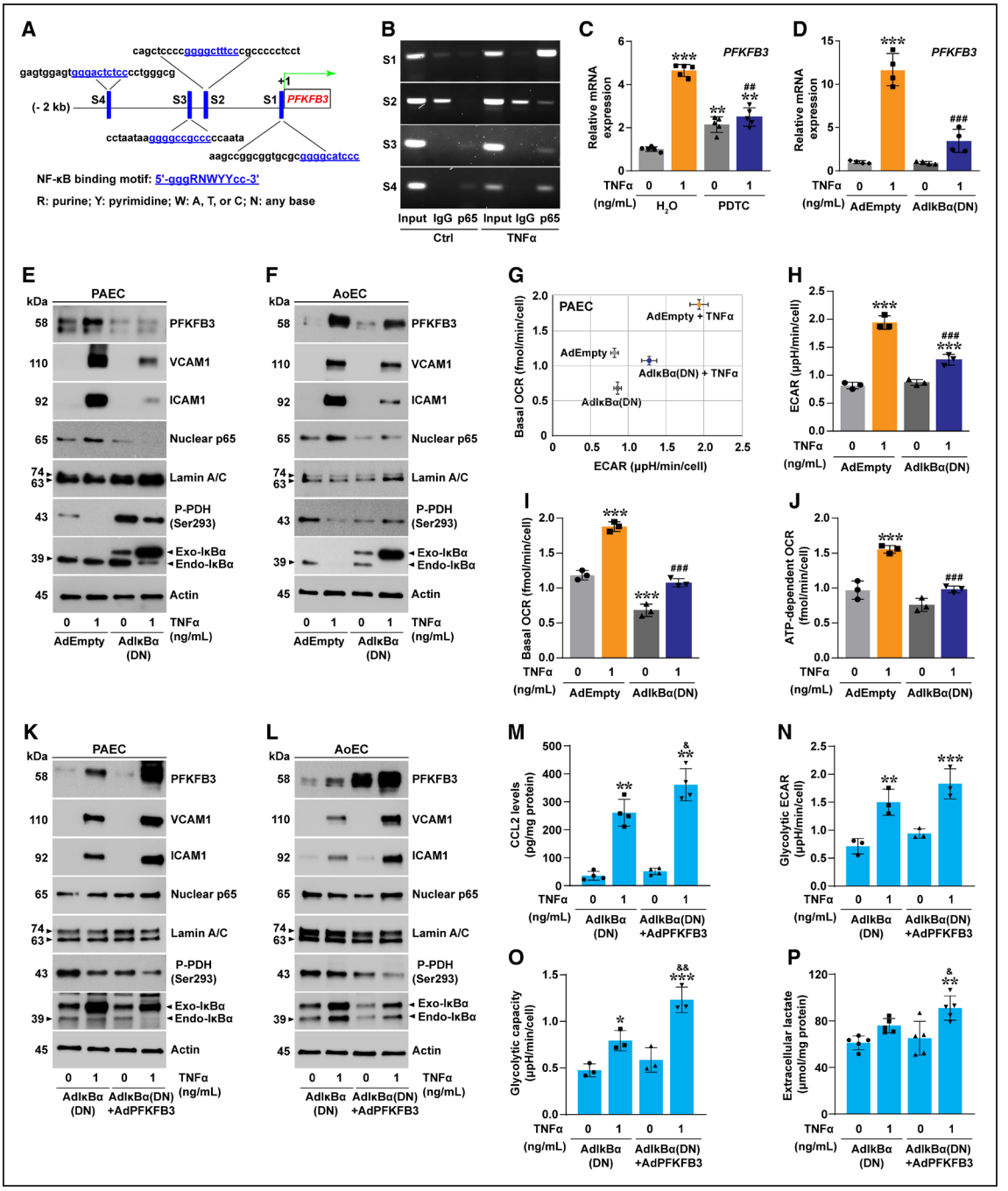

Figure 6. The NF-κB (nuclear factor-kappa B)–PFKFB3 (6-phosphofructo-2-kinase/fructose 2,6-bisphosphatase 3) axis promotes glycolysis and inflammation.

A, Bioinformatic identification of 4 potential binding sites (S1–S4) of NF-κB (p65) at the promoter region of human *PFKFB3* gene. **B**, ChIP (chromatin immunoprecipitation) assay shows the binding of p65 protein to the *PFKFB3* promoter with or without TNFα (tumor necrosis factor alpha) stimulation (1 ng/mL for 4 h); n=3. **C** and **D**, *PFKFB3* mRNA expression in pulmonary artery endothelial cells (PAECs) with NF-κB pathway inactivation by PDTC (50 μM; **C**; n=5) or overexpression of a dominant-negative IκBα (IkappaBalpha) protein (AdIκBα[DN]; 20 MOI; **D**; n=4) followed by TNFα stimulation for 4 h. **E** and **F**, Immunoblotting images showing the levels of inflammatory and metabolic proteins in PAECs (**E**) or aortic endothelial cells (AoECs; **F**) transfected with AdEmpty or AdIκBα(DN) followed by TNFα stimulation; n=3. **G**, Energetics map from the Seahorse mitochondrial stress test showing basal oxygen consumption rate (OCR) and extracellular acidification rate (ECAR) in PAECs with 24 h of TNFα treatment; n=3. **H**–**J**, Quantitation of ECAR (**H**), basal OCR (**I**), and ATP-dependent OCR (**J**) from the Seahorse assay; n=3. **K** and **L**, Immunoblots showing the levels of inflammatory and metabolic proteins in PAECs (**K**) or AoECs (**L**) transfected with AdIκBα(DN) or cotransfected with AdIκBα(DN) and AdPFKFB3 followed by TNFα stimulation for 24 h; n=3. **M**, CCL2 (C-C motif chemokine ligand 2) levels in PAECs with the same treatment as in panel K; n=4. **N** and **O**, Seahorse glycolysis stress test shows glycolytic ECAR (**N**) and capacity (**O**) in PAECs; n=3. **P**, Extracellular lactate levels in PAECs determined by a fluorescence-based assay; n=5. Data presented as mean±SD. **P*<0.05, ***P*<0.01, ****P*<0.001 vs control by the Kruskal-Wallis test followed by Dunn test (**C**, **D**, **H**–**J**, and **M**–**P**); ##*P*<0.01 and ###*P*<0.001 vs H_2O-treated or AdEmpty-transfected cells with TNFα stimulation by Dunn test (**C**, **D** and **H**–**J**); &*P*<0.05 and &&*P*<0.01 vs AdIκBα-transfected cells with TNFα stimulation by Dunn test (**M**, **O**, and **P**).

in the Data Supplement). Blockade of NF-κB signaling also completely abolished TNFα-stimulated increases in basal and ATP-dependent OCR in ECs (Figure 6I and 6J; Figure IVL and IVM in the Data Supplement), which were accompanied by significant recovery of the reduced P-PDH protein levels (Figure 6E and 6F). Therefore, together with the findings in Figure 5 showing PFKFB3 upregulation enhances glycolysis to promote inflammation, these results indicate that the normalization of PFKFB3-mediated enhancement of glycolysis could be a possible mechanism mediating the anti-inflammatory effects of NF-κB inhibition in ECs.

To test further the causality of PFKFB3 in mediating such immunometabolic effects, we overexpressed *PFKFB3* in ECs with co-overexpression of IκBα(DN) protein followed by TNFα stimulation. Immunoblotting assays showed that overexpression of *PFKFB3* was sufficient to offset significantly the inhibitory effects of NF-κB blockade on VCAM1, ICAM1, and CCL2 protein expression, which correlated with a significant potentiation of elevated PFKFB3 protein and a slight augmentation of nuclear translocation of p65 protein in inflamed ECs (Figure 6K through 6M). We then tested the metabolic responses in the same setting. Results from the Seahorse assay showed that in the presence of TNFα, PAECs with both PFKFB3 and IκBα(DN) overexpression exhibited much lower OCR than cells with IκBα(DN) overexpression alone (Figure VIN through VIQ in the Data Supplement), which seemed to be independent of the aggravated reduction in P-PDH protein levels in ECs (Figure 6K and 6L) since lower P-PDH protein is expected to increase its activity and, thus, oxygen consumption. Nevertheless, overexpression of *PFKFB3* was, indeed, sufficient to sustain the TNFα-induced increase in glycolytic activity as evidenced by potentiated increases in glycolytic ECAR (to a lesser extent), glycolytic capacity, and LAC secretion in PAECs with IκBα(DN) and PFKFB3 co-overexpression (Figure 6N through 6P), which correlated with the recovery of proinflammatory adhesion proteins (Figure 6K through 6M). Hence, PFKFB3 is an essential regulator mediating the NF-κB inactivation–induced suppression of glycolysis and inflammation in ECs. Taken together, these data indicate that the NF-κB–PFKFB3 axis promotes glycolysis and inflammation and that blockade of PFKFB3-induced stimulation of glycolysis by NF-κB inactivation is a novel anti-inflammatory mechanism in human arterial ECs.

Perturbation of Glucose Metabolism Modulates Mesenteric Vessel Inflammation In Vivo

Lastly, we examined the in vivo relevance of these in vitro findings and tested whether manipulating glucose metabolism could regulate endothelial inflammation in mesenteric vessels of LPS-treated mice. To this end, glycolysis and the PPP were inhibited by inactivation of their corresponding key regulatory enzymes, PFKFB3 and G6PD, with the pharmacological inhibitors 3-PO and DHEA, respectively, while mitochondrial OXPHOS was enhanced by blockade of PDKs using the pharmacological antagonist DCA (Figure 7A). Following these pretreatments, LPS was injected intraperitoneally to induce sepsis-like inflammation in mice (Figure 7A). We first confirmed that, consistent with the in vitro observations in Figure 2, LPS stimulated PFKFB3 and G6PD expression and reduced P-PDH levels in mesenteric vessels in vivo (Figure VII in the Data Supplement). Interestingly, administration of 3-PO unexpectedly diminished the LPS-induced elevation of PFKFB3 protein levels in mesenteric vessels, albeit DHEA pretreatment did not affect G6PD expression in vivo (Figure VII in the Data Supplement). The P-PDH protein levels were reduced by 30% in mesenteric vessels of mice pretreated with DCA alone, and, importantly, such pretreatment further decreased the LPS-induced reduction of P-PDH levels by 15% (Figure VII in the Data Supplement), indicating that DCA is effective in suppressing PDK activity in our model.

Intravital microscopy analysis showed that LPS treatment increased the numbers of both rolling and adherent leukocytes in mesenteric venules, both of which were also observed in mice treated with the G6PD inhibitor DHEA alone (Figure 7B through 7D). Of note, pretreatment with DHEA further enhanced LPS-induced increases in leukocyte rolling and adhesion in mesenteric venules; in sharp contrast, such increases in LPS-stimulated mice were significantly normalized by pretreatment with 3-PO or DCA (Figure 7B through 7D). These results indicate that LPS-induced inflammation could be potentiated by DHEA and attenuated by 3-PO and DCA in mesenteric vessels in vivo.

Since the interaction of circulating leukocytes with the endothelium is finely tuned by adhesion molecules, known targets of the inflammatory mediators used in these experiments, we measured vessel VCAM1 expression and plasma E-selectin and P-selectin levels. As anticipated, LPS stimulation significantly upregulated VCAM1 expression in mesenteric vessels and increased plasma E-selectin and P-selectin levels (Figure 7E through 7H). Strikingly, 3-PO or DCA pretreatment normalized LPS-induced upregulation of vessel VCAM1 expression and elevations in plasma E-selectin and P-selectin levels (Figure 7E through 7H). By contrast, DHEA pretreatment alone increased plasma P-selectin levels (Figure 7H). Such pretreatment further potentiated LPS-induced secretion of P-selectin, although it failed to influence significantly LPS-induced elevations of the other two adhesion molecules (Figure 7E through 7H). Thus, in keeping with our in vitro findings (Figures 3 through 6), these in vivo results also indicate that inhibition of the PPP potentiates mesenteric vessel

ORIGINAL RESEARCH

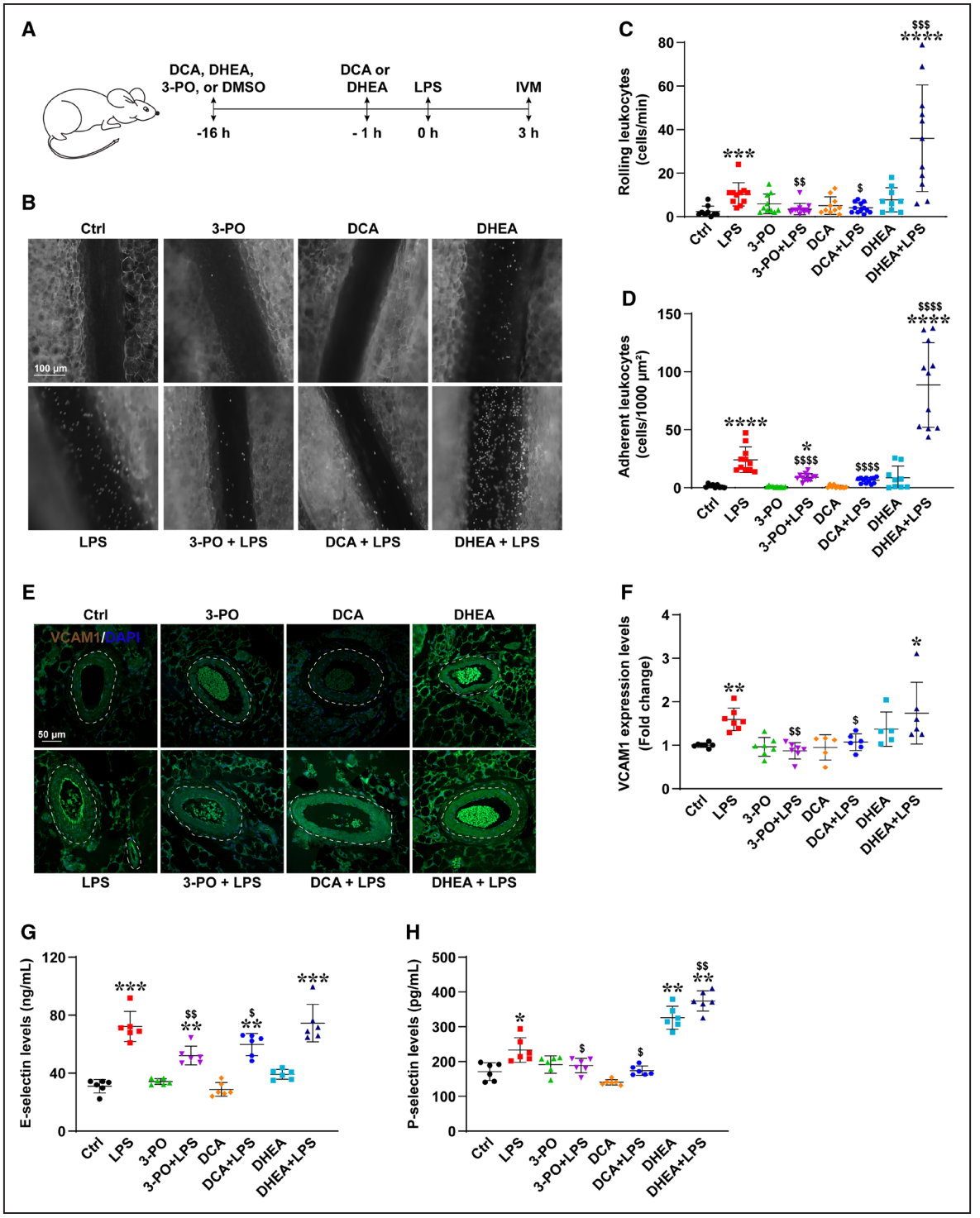

Figure 7. Modulating glucose metabolism regulates mesenteric vessel inflammation in lipopolysaccharide (LPS)-stimulated mice.

A, Schematic illustration of the treatment protocol for intravital microscopy (IVM). **B**, Representative IVM images showing the adhesion of leukocytes to the mesenteric endothelium. Scale, 100 μm. **C** and **D**, Quantitative IVM results of rolling leukocytes (**C**) and adherent leukocytes (**D**); n=9 in Ctrl and DHEA groups, n=10 in 3-PO and DCA groups, n=11 in LPS and DHEA+LPS groups, n=12 in 3-PO+LPS and DCA+LPS groups. **E** and **F**, Immunofluorescent images (**E**) and corresponding quantitation (**F**) of VCAM1 (vascular cell adhesion molecule 1) expression on mesenteric vessels; n=5 in DCA and DHEA groups, n=6 in DCA+LPS and DHEA+LPS groups, n=7 in other groups. Scale, 50 μm. **G** and **H**, ELISA measurements of plasma E-selectin (**G**) and P-selectin (**H**) levels; n=6. Data presented as mean±SD. **P*<0.05, ***P*<0.01, ****P*<0.001, *****P*<0.0001 vs vehicle control (Ctrl) treated mice by 1-way ANOVA followed by Tukey test (**C** and **D**) or the Kruskal-Wallis test followed by Dunn test (**F**–**H**); $*P*<0.05, $$*P*<0.01, $$$*P*<0.001, and $$$$*P*<0.0001 vs LPS-stimulated mice by Tukey test (**C** and **D**) or Dunn test (**F**–**H**).

inflammation, while blockade of glycolysis or enhancement of OXPHOS attenuates the inflammatory response in the mesenteric endothelium.

DISCUSSION

Here, we demonstrate that the immunometabolic phenotype of the endothelium is dynamic and adaptive, and that cellular metabolism is reprogrammed in response to inflammatory stimulation in ECs. Specifically, inflammatory stimuli activate glycolysis, mitochondrial OXPHOS, and the PPP. While blocking the enhancement of mitochondrial OXPHOS and the PPP leads to potentiation of inflammation, inhibiting the enhancement of glycolysis attenuates inflammation. Therefore, we conclude that mitochondrial OXPHOS and the PPP are activated as homeostatic anti-inflammatory mechanisms, whereas the enhancement of glycolysis promotes inflammatory responses in vascular ECs in vitro and in vivo (Figure 8).

Surprisingly, such integrative metabolic information has been very limited in normal ECs. Drabarek et al[38] reported that TNFα enhances oxygen consumption and mitochondrial biogenesis in the human EC line EA.hy926, indicating an increase in mitochondrial respiration. A recent study showed that LPS stimulation significantly increased glycolytic ECAR and LAC levels in PAECs, implying stimulation of glycolysis.[39] However, neither study characterized the influence of TNFα or LPS on the complementary metabolic pathways for glucose, each focusing exclusively on one pathway. To the best of our knowledge, we show here for the first time that inflammatory stimuli enhance all 3 key branches of central glucose metabolism in human primary arterial ECs.

We also provide critical evidence in support of the principal enzymes responsible for this immunometabolic reprogramming. The entry of glucose-derived PYR into the TCA cycle is finely tuned by the PDH complex, which can be phosphorylated and inactivated by PDK enzymes (PDK1–4).[27] We found that the enhanced mitochondrial OXPHOS was largely mediated by downregulation of PDK4 and P-PDH levels since overexpression of *PDK4* significantly recovered the suppression of PDK4 and P-PDH expression and attenuated the elevated OCR in PAECs exposed to inflammatory stimuli. By sharp contrast, Park and Jeoung[25] reported that LPS induced *PDK4* mRNA and protein expression resulting in a decrease in PDH activity and a metabolic shift from mitochondrial OXPHOS to glycolysis in C2C12 myoblasts, highlighting responses unique to ECs in our experiments. Mechanistically, we found that inflammatory stimuli-induced *PDK4* downregulation is mediated by inhibition of FOXO1—a known transcriptional activator of PDK4.[30] Previous

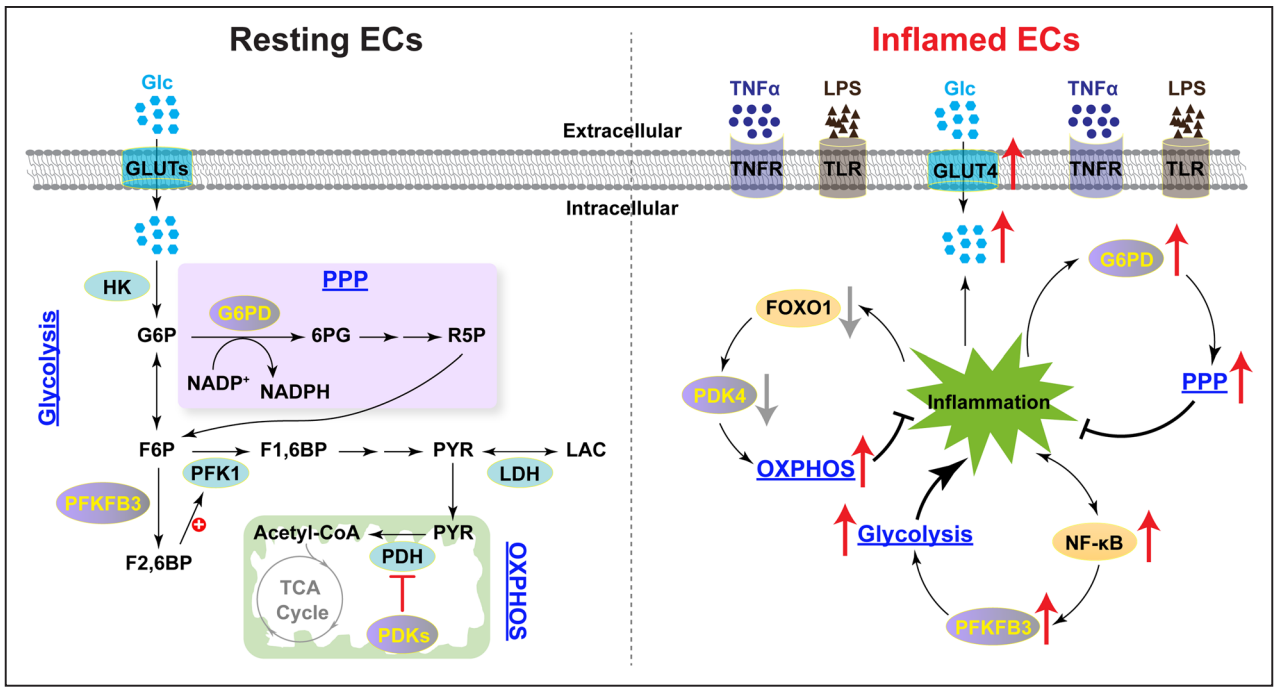

Figure 8. Proposed immunometabolic regulation of resting and inflamed endothelial cell (EC) phenotypes.
In resting ECs, the 3 central glucose metabolism pathways of glycolysis, the pentose phosphate pathway (PPP), and mitochondrial oxidative phosphorylation (OXPHOS) are active. PFKFB3 (6-phosphofructo-2-kinase/fructose 2,6-bisphosphatase 3) maintains glycolysis by generating F2,6BP as a potent agonist of the rate-limiting enzyme PFK1 (phosphofructokinase 1). G6PD (glucose 6-phosphate dehydrogenase) is the first and rate-limiting enzyme of the PPP. PDKs govern the flux of glucose-derived pyruvate into the tricarboxylic acid cycle and OXPHOS via phosphorylation and inactivation of PDH complex. Upon inflammatory stimulation, all 3 glucose metabolism pathways are extensively enhanced in ECs. In turn, enhanced PPP and mitochondrial OXPHOS via upregulation of G6PD or inhibition of the FOXO1 (forkhead box O1)-PDK4 (pyruvate dehydrogenase kinase 4) axis, respectively, suppress inflammation, while heightened glycolysis via activation of the NF-κB (nuclear factor-kappa B)–PFKFB3 pathway promotes inflammation.

studies revealed that TNFα inhibited FOXO1 expression and transcriptional activity through NF-κB–dependent upregulation of miR-705 in mouse bone marrow–derived mesenchymal stem cells[40] and through PI3K (phosphatidylinositol 3-kinase)- and IKK2 (IκB kinase 2)-mediated phosphorylation of FOXO1 in human pulmonary arterial smooth muscle cells.[41] Whether or not these mechanisms contribute to the repression of FOXO1 in inflamed ECs remains to be determined. Notably, we also demonstrated that overexpression of *FOXO1* restored the reductions of *PDK4* and P-PDH expression and recapitulated the metabolic effects of *PDK4* overexpression in TNFα- or LPS-treated ECs. In line with our findings, overexpression of *FOXO1* transcriptionally activated PDK4 and, thereby, reduced PDH activity in mouse cardiomyocytes; by contrast, pharmacological and genetic inactivation of FOXO1 repressed PDK4 expression and P-PDH protein levels.[42] Thus, the FOXO1-PDK4 axis is essential in controlling mitochondrial respiration uniquely in ECs; blockade of this axis results in elevated mitochondrial OXPHOS in ECs exposed to inflammatory stimuli.

Enhanced glycolysis was associated with upregulation of PFKFB3, HK2, PKM2, and LDHA expression in ECs. Unlike the response of other glycolytic genes, the upregulation of PFKFB3 expression was robust and consistent for PAECs and AoECs with TNFα or LPS treatment. Using loss- and gain-of-function studies of *PFKFB3*, we clearly demonstrated that PFKFB3 is a crucial enzyme mediating the enhancement in glycolysis under inflammation and that *PFKFB3* knockdown induces a metabolic shift from glycolysis to mitochondrial OXPHOS. In support of this view, Wang et al[39] showed that LPS upregulated PFKFB3 expression and activity leading to enhancement of glycolysis in PAECs, which was abrogated by *PFKFB3* silencing. In HUVECs with *PFKFB3* silencing, a metabolic switch from glycolysis to the PPP and fatty acid oxidation rather than glucose oxidation was observed.[7] By contrast, several studies demonstrated disturbed/low shear stress–induced aerobic activation of HIF-1α signaling and consequent upregulation of PFKFB3, resulting in a metabolic shift to glycolysis in human AoECs and HUVECs.[43,44] Collectively, evidence from our study and others clearly supports the view that PFKFB3 is the principal regulatory enzyme of glycolysis, including in the setting of inflammation, and that inhibition of PFKFB3 reprograms cellular metabolism in ECs.

How increased mitochondrial respiration modulates inflammation in ECs remained unknown until recently. Here, we found that mitochondrial respiration may be enhanced as a counterregulatory anti-inflammatory response in vitro and in vivo through inhibition of the FOXO1-PDK4 axis. In support of this view, Wu et al[44] reported that disturbed flow inhibited mitochondrial respiration via aerobic activation of HIF-1α–PDK1 signaling leading to inflammation in human AoECs. This proinflammatory phenotype was normalized when mitochondrial respiration was recovered by inactivation of this specific pathway.[44] In macrophages, inhibition of PDK2 and PDK4 enhanced mitochondrial glucose oxidation and prevented LPS/IFN-γ (interferon gamma)–induced proinflammatory M1 polarization and cytokine secretion, which correlated with an amelioration of inflammation in adipose tissues of high fat diet–fed mice in vivo.[45] Interestingly, overexpression of dominant-negative *FOXO1* in mouse tibialis anterior muscle decreased glucose uptake in vivo and protein levels of mitochondrial respiratory complexes I–V, implying a suppression of mitochondrial glucose oxidation; these changes were accompanied by a proinflammatory response and activation of mTOR and AKT signaling pathways.[46] Furthermore, in Fawn-hooded rats with spontaneously developed PAH, right ventricular tissue expressed higher levels of PDK4 and FOXO1 proteins, which correlated with a decrease in PDH activity and a metabolic switch from mitochondrial OXPHOS to glycolysis.[24] Of note, such molecular, metabolic, and pathobiological alterations in cardiac tissue of these PAH rats were significantly corrected by treatment with DCA,[24] indicating that DCA can block the FOXO1-PDK4 axis leading to restoration of PDH activity and, thereby, enhancement of glucose oxidation. Here, we demonstrate for the first time that the enhancement of mitochondrial respiration due to inhibition of the FOXO1-PDK4 axis is an anti-inflammatory homeostatic response in human arterial ECs, although the precise underlying mechanisms mediating this anti-inflammatory effect remain to be explored.

Likewise, we also demonstrated that blockade of the PPP by inhibition of G6PD markedly augmented endothelial inflammatory response in vitro and in vivo, supporting the view that G6PD-mediated stimulation of the PPP is also a counterregulatory anti-inflammatory response. The PPP is a primary source of cytosolic reducing equivalents.[32] As expected, G6PD inhibition alone decreased cellular NADPH and GSH levels, which correlated with elevation of reactive oxygen species production and upregulation of endothelial inflammatory adhesion molecules. Thus, we speculated that the potentiated inflammation induced by G6PD inactivation may be mediated by oxidative stress. In accordance with our speculation, 2 independent studies reported that *G6PD* silencing or deficiency further exacerbated inflammatory responses and, importantly, that these effects were abrogated by pretreatment with GSH precursors (eg, N-acetyl-*L*-cysteine), supporting the view that oxidative stress mediates these biological changes.[47,48] Surprisingly, the potentiation of inflammation we observed in *G6PD*-silenced PAECs appeared to be only partly related to oxidative stress, with a greater dependence on the potentiation of PFKFB3 upregulation and consequently metabolic reprogramming to glycolysis. This metabolic shift to glycolysis can minimize reactive oxygen species generation

by the mitochondrial respiratory chain, which, in part, may also explain the normalization of oxidative stress in *G6PD* silenced and inflamed cells. Collectively, blockade of the PPP by G6PD inhibition reprograms cellular metabolism to glycolysis and potentiates inflammation.

The hypothesis that glycolysis promotes inflammation was supported by in vivo evidence that PFKFB3 inactivation by 3-PO normalized LPS-induced mesenteric endothelial inflammation and by in vitro evidence that PFKFB3 inhibition or overexpression attenuated or exacerbated the enhancement of glycolysis and inflammation in inflamed ECs, respectively. Of note, the expression patterns of *LDHA* and *PKM2* were not significantly affected by PFKFB3 manipulation, further supporting that PFKFB3 is the key enzyme mediating these immunometabolic effects in ECs. Accumulating evidence supports such a role for PFKFB3 in inflammation. For example, genetic or pharmacological inhibition of PFKFB3 significantly ameliorates TNFα- or IL-1β–induced the upregulation and secretion of inflammatory markers and the monocyte adhesion to and migration through ECs.[49,50] In an LPS-induced acute lung injury mouse model, endothelial-specific deletion of *PFKFB3* abrogated LPS-induced infiltration of immune cells in the lungs and upregulation of cytokines and adhesion molecules.[39] Consistent with our observations, these authors also reported that silencing *PFKFB3* abrogated LPS-induced stimulation of glycolysis and inflammation in PAECs.[39] Furthermore, silencing *PFKFB3* normalized the glycolytic phenotype of primary PAECs isolated from idiopathic PAH patients, which correlated with repressed expression of inflammatory markers.[51] Taken together, these data support the conclusion that the PFKFB3-induced enhancement of glycolysis is a general mechanism that promotes inflammation.

Mechanistically, previous studies reported that inhibition of PFKFB3 normalized inflammation in ECs through blocking nuclear translocation of p65 protein and reducing transcriptional activity of the NF-κB signaling.[39,49,50,52] Our results show that *PFKFB3* or *PKM2* silencing partially abrogated the increase in total cellular p65 protein levels in inflamed PAECs—a finding not observed previously.[39,50,52] We also observed a metabolic switch to mitochondrial OXPHOS, with an accompanying anti-inflammatory response, in *PFKFB3*-silenced ECs. Thus, these lines of evidence indicate that blockade of NF-κB signaling and the metabolic shift to OXPHOS could, in part, explain the anti-inflammatory effects of PFKFB3 inactivation. More intriguingly, we identified that *PFKFB3* is a previously unrecognized transcriptional target of NF-κB signaling. These findings support a reciprocal regulatory mechanism between NF-κB signaling and PFKFB3 in the setting of EC inflammation. Importantly, the immunometabolic functions of NF-κB–PFKFB3 signaling had previously been unrecognized. Here, we demonstrate that inactivation of NF-κB signaling suppresses the inflammatory response through normalizing PFKFB3 upregulation and, thus, attenuating the enhanced glycolysis. Therefore, inhibition of the NF-κB–PFKFB3 signaling axis is also a novel anti-inflammatory mechanism in human arterial ECs.

In conclusion, we demonstrate that the key metabolic pathways of glucose distinctly modulate endothelial inflammation in vitro and in vivo, are themselves modulated by inflammatory stimuli, and define immunometabolic EC phenotypes. The enhancement of mitochondrial respiration and the PPP are counterregulatory anti-inflammatory responses, while the NF-κB–PFKFB3 signaling–mediated stimulation of glycolysis promotes inflammation. Knowledge gained from this study provides insight into fundamental mechanisms underlying immunometabolic interactions in a unique cell type essential to the inflammatory response, and may offer a novel rationale for developing metabolic therapeutic strategies for the treatment of inflammatory disorders.

ARTICLE INFORMATION

Received December 29, 2020; revision received April 16, 2021; accepted April 22, 2021.

Affiliation

Division of Cardiovascular Medicine (W.X., A.K.P., J.L.) and Division of Pulmonary and Critical Care Medicine, Department of Medicine (W.M.O., C.P.), Brigham and Women's Hospital and Harvard Medical School, Boston, MA.

Acknowledgments

We acknowledge Dr Robert Flaumenhaft and Glenn Merrill-Skoloff (Beth Israel Deaconess Medical Center) for kindly providing access to their intravital microscope. We thank Dr Diane E. Handy for the IκBα (IkappaBalpha) adenoviral vector and Dr Domenico Accili (Columbia University) for the mouse FOXO1 (forkhead box O1) adenoviral vector. We also thank Ashish Gurung for technical support on [^{14}C]-CO_2 release assay and Stephanie Tribuna for assistance in preparation of this manuscript.

Sources of Funding

This work is supported by the National Institutes of Health (NIH) grants HG007690, HL061795, HL119145, HL155107, and GM107618 and the American Heart Association grants D700382 and CV-19 to J. Loscalzo and NIH grant HL128802 to W.M. Oldham.

Disclosures

None.

Supplemental Materials

Expanded Methods and Materials
Data Supplement Figures I–VII
Data Supplement Tables I–III and V
References [1,37,49,53–71]

REFERENCES

1. Cines DB, Pollak ES, Buck CA, Loscalzo J, Zimmerman GA, McEver RP, Pober JS, Wick TM, Konkle BA, Schwartz BS, et al. Endothelial cells in physiology and in the pathophysiology of vascular disorders. *Blood.* 1998;91:3527–3561.
2. Favero G, Paganelli C, Buffoli B, Rodella LF, Rezzani R. Endothelium and its alterations in cardiovascular diseases: life style intervention. *Biomed Res Int.* 2014;2014:801896. doi: 10.1155/2014/801896

3. Dobrina A, Rossi F. Metabolic properties of freshly isolated bovine endothelial cells. *Biochim Biophys Acta*. 1983;762:295–301. doi: 10.1016/0167-4889(83)90084-8
4. Spolarics Z, Spitzer JJ. Augmented glucose use and pentose cycle activity in hepatic endothelial cells after in vivo endotoxemia. *Hepatology*. 1993;17:615–620. doi: 10.1002/hep.1840170415
5. Culic O, Gruwel ML, Schrader J. Energy turnover of vascular endothelial cells. *Am J Physiol*. 1997;273:C205–C213. doi: 10.1152/ajpcell.1997.273.1.C205
6. Krützfeldt A, Spahr R, Mertens S, Siegmund B, Piper HM. Metabolism of exogenous substrates by coronary endothelial cells in culture. *J Mol Cell Cardiol*. 1990;22:1393–1404. doi: 10.1016/0022-2828(90)90984-a
7. De Bock K, Georgiadou M, Schoors S, Kuchnio A, Wong BW, Cantelmo AR, Quaegebeur A, Ghesquière B, Cauwenberghs S, Eelen G, et al. Role of PFKFB3-driven glycolysis in vessel sprouting. *Cell*. 2013;154:651–663. doi: 10.1016/j.cell.2013.06.037
8. De Bock K, Georgiadou M, Carmeliet P. Role of endothelial cell metabolism in vessel sprouting. *Cell Metab*. 2013;18:634–647. doi: 10.1016/j.cmet.2013.08.001
9. Sprague AH, Khalil RA. Inflammatory cytokines in vascular dysfunction and vascular disease. *Biochem Pharmacol*. 2009;78:539–552. doi: 10.1016/j.bcp.2009.04.029
10. Lusis AJ. Atherosclerosis. *Nature*. 2000;407:233–241. doi: 10.1038/35025203
11. Schermuly RT, Ghofrani HA, Wilkins MR, Grimminger F. Mechanisms of disease: pulmonary arterial hypertension. *Nat Rev Cardiol*. 2011;8:443–455. doi: 10.1038/nrcardio.2011.87
12. Rabinovitch M, Guignabert C, Humbert M, Nicolls MR. Inflammation and immunity in the pathogenesis of pulmonary arterial hypertension. *Circ Res*. 2014;115:165–175. doi: 10.1161/CIRCRESAHA.113.301141
13. Weber C, Noels H. Atherosclerosis: current pathogenesis and therapeutic options. *Nat Med*. 2011;17:1410–1422. doi: 10.1038/nm.2538
14. Pircher A, Treps L, Bodrug N, Carmeliet P. Endothelial cell metabolism: a novel player in atherosclerosis? Basic principles and therapeutic opportunities. *Atherosclerosis*. 2016;253:247–257. doi: 10.1016/j.atherosclerosis.2016.08.011
15. Sutendra G, Michelakis ED. The metabolic basis of pulmonary arterial hypertension. *Cell Metab*. 2014;19:558–573. doi: 10.1016/j.cmet.2014.01.004
16. Xu W, Koeck T, Lara AR, Neumann D, DiFilippo FP, Koo M, Janocha AJ, Masri FA, Arroliga AC, Jennings C, et al. Alterations of cellular bioenergetics in pulmonary artery endothelial cells. *Proc Natl Acad Sci USA*. 2007;104:1342–1347. doi: 10.1073/pnas.0605080104
17. Xu W, Erzurum SC. Endothelial cell energy metabolism, proliferation, and apoptosis in pulmonary hypertension. *Compr Physiol*. 2011;1:357–372. doi: 10.1002/cphy.c090005
18. Soon E, Holmes AM, Treacy CM, Doughty NJ, Southgate L, Machado RD, Trembath RC, Jennings S, Barker L, Nicklin P, et al. Elevated levels of inflammatory cytokines predict survival in idiopathic and familial pulmonary arterial hypertension. *Circulation*. 2010;122:920–927. doi: 10.1161/CIRCULATIONAHA.109.933762
19. Divakaruni AS, Paradyse A, Ferrick DA, Murphy AN, Jastroch M. Analysis and interpretation of microplate-based oxygen consumption and pH data. *Methods Enzymol*. 2014;547:309–354. doi: 10.1016/B978-0-12-801415-8.00016-3
20. Mookerjee SA, Goncalves RLS, Gerencser AA, Nicholls DG, Brand MD. The contributions of respiration and glycolysis to extracellular acid production. *Biochim Biophys Acta*. 2015;1847:171–181. doi: 10.1016/j.bbabio.2014.10.005
21. Eelen G, de Zeeuw P, Simons M, Carmeliet P. Endothelial cell metabolism in normal and diseased vasculature. *Circ Res*. 2015;116:1231–1244. doi: 10.1161/CIRCRESAHA.116.302855
22. Kalucka J, de Rooij LPMH, Goveia J, Rohlenova K, Dumas SJ, Meta E, Conchinha NV, Taverna F, Teuwen LA, Veys K, et al. Single-cell transcriptome atlas of murine endothelial cells. *Cell*. 2020;180:764.e20–779.e20. doi: 10.1016/j.cell.2020.01.015
23. Corcoran CC, Grady CR, Pisitkun T, Parulekar J, Knepper MA. From 20th century metabolic wall charts to 21st century systems biology: database of mammalian metabolic enzymes. *Am J Physiol Renal Physiol*. 2017;312:F533–F542. doi: 10.1152/ajprenal.00601.2016
24. Piao L, Sidhu VK, Fang YH, Ryan JJ, Parikh KS, Hong Z, Toth PT, Morrow E, Kutty S, Lopaschuk GD, et al. FOXO1-mediated upregulation of pyruvate dehydrogenase kinase-4 (PDK4) decreases glucose oxidation and impairs right ventricular function in pulmonary hypertension: therapeutic benefits of dichloroacetate. *J Mol Med (Berl)*. 2013;91:333–346. doi: 10.1007/s00109-012-0982-0
25. Park H, Jeoung NH. Inflammation increases pyruvate dehydrogenase kinase 4 (PDK4) expression via the Jun N-Terminal Kinase (JNK) pathway in C2C12 cells. *Biochem Biophys Res Commun*. 2016;469:1049–1054. doi: 10.1016/j.bbrc.2015.12.113
26. Okar DA, Manzano A, Navarro-Sabatè A, Riera L, Bartrons R, Lange AJ. PFK-2/FBPase-2: maker and breaker of the essential biofactor fructose-2,6-bisphosphate. *Trends Biochem Sci*. 2001;26:30–35. doi: 10.1016/s0968-0004(00)01699-6
27. Zhang S, Hulver MW, McMillan RP, Cline MA, Gilbert ER. The pivotal role of pyruvate dehydrogenase kinases in metabolic flexibility. *Nutr Metab (Lond)*. 2014;11:10. doi: 10.1186/1743-7075-11-10
28. Wang D, Wang Q, Yan G, Qiao Y, Zhu B, Liu B, Tang C. Hypoxia induces lactate secretion and glycolytic efflux by downregulating mitochondrial pyruvate carrier levels in human umbilical vein endothelial cells. *Mol Med Rep*. 2018;18:1710–1717. doi: 10.3892/mmr.2018.9079
29. Vats D, Mukundan L, Odegaard JI, Zhang L, Smith KL, Morel CR, Wagner RA, Greaves DR, Murray PJ, Chawla A. Oxidative metabolism and PGC-1beta attenuate macrophage-mediated inflammation. *Cell Metab*. 2006;4:13–24. doi: 10.1016/j.cmet.2006.05.011
30. Furuyama T, Kitayama K, Yamashita H, Mori N. Forkhead transcription factor FOXO1 (FKHR)-dependent induction of PDK4 gene expression in skeletal muscle during energy deprivation. *Biochem J*. 2003;375:365–371. doi: 10.1042/BJ20030022
31. Leopold JA, Cap A, Scribner AW, Stanton RC, Loscalzo J. Glucose-6-phosphate dehydrogenase deficiency promotes endothelial oxidant stress and decreases endothelial nitric oxide bioavailability. *FASEB J*. 2001;15:1771–1773. doi: 10.1096/fj.00-0893fje
32. Xiao W, Wang RS, Handy DE, Loscalzo J. NAD(H) and NADP(H) redox couples and cellular energy metabolism. *Antioxid Redox Signal*. 2018;28:251–272. doi: 10.1089/ars.2017.7216
33. Xiao W, Loscalzo J. Metabolic responses to reductive stress. *Antioxid Redox Signal*. 2020;32:1330–1347. doi: 10.1089/ars.2019.7803
34. Clem B, Telang S, Clem A, Yalcin A, Meier J, Simmons A, Rasku MA, Arumugam S, Dean WL, Eaton J, et al. Small-molecule inhibition of 6-phosphofructo-2-kinase activity suppresses glycolytic flux and tumor growth. *Mol Cancer Ther*. 2008;7:110–120. doi: 10.1158/1535-7163.MCT-07-0482
35. Clem BF, O'Neal J, Tapolsky G, Clem AL, Imbert-Fernandez Y, Kerr DA 2nd, Klarer AC, Redman R, Miller DM, Trent JO, et al. Targeting 6-phosphofructo-2-kinase (PFKFB3) as a therapeutic strategy against cancer. *Mol Cancer Ther*. 2013;12:1461–1470. doi: 10.1158/1535-7163.MCT-13-0097
36. Kao DD, Oldebeken SR, Rai A, Lubos E, Leopold JA, Loscalzo J, Handy DE. Tumor necrosis factor-α-mediated suppression of dual-specificity phosphatase 4: crosstalk between NFκB and MAPK regulates endothelial cell survival. *Mol Cell Biochem*. 2013;382:153–162. doi: 10.1007/s11010-013-1730-7
37. Brockman JA, Scherer DC, McKinsey TA, Hall SM, Qi X, Lee WY, Ballard DW. Coupling of a signal response domain in I kappa B alpha to multiple pathways for NF-kappa B activation. *Mol Cell Biol*. 1995;15:2809–2818. doi: 10.1128/mcb.15.5.2809
38. Drabarek B, Dymkowska D, Szczepanowska J, Zabłocki K. TNFα affects energy metabolism and stimulates biogenesis of mitochondria in EA.hy926 endothelial cells. *Int J Biochem Cell Biol*. 2012;44:1390–1397. doi: 10.1016/j.biocel.2012.05.022
39. Wang L, Cao Y, Gorshkov B, Zhou Y, Yang Q, Xu J, Ma Q, Zhang X, Wang J, Mao X, et al. Ablation of endothelial Pfkfb3 protects mice from acute lung injury in LPS-induced endotoxemia. *Pharmacol Res*. 2019;146:104292. doi: 10.1016/j.phrs.2019.104292
40. Liao L, Su X, Yang X, Hu C, Li B, Lv Y, Shuai Y, Jing H, Deng Z, Jin Y. TNF-α inhibits FoxO1 by upregulating miR-705 to aggravate oxidative damage in bone marrow-derived mesenchymal stem cells during osteoporosis. *Stem Cells*. 2016;34:1054–1067. doi: 10.1002/stem.2274
41. Savai R, Al-Tamari HM, Sedding D, Kojonazarov B, Muecke C, Teske R, Capecchi MR, Weissmann N, Grimminger F, Seeger W, et al. Pro-proliferative and inflammatory signaling converge on FoxO1 transcription factor in pulmonary hypertension. *Nat Med*. 2014;20:1289–1300. doi: 10.1038/nm.3695
42. Gopal K, Saleme B, Al Batran R, Aburasayn H, Eshreif A, Ho KL, Ma WK, Almutairi M, Eaton F, Gandhi M, et al. FoxO1 regulates myocardial glucose oxidation rates via transcriptional control of pyruvate dehydrogenase kinase 4 expression. *Am J Physiol Heart Circ Physiol*. 2017;313:H479–H490. doi: 10.1152/ajpheart.00191.2017
43. Feng S, Bowden N, Fragiadaki M, Souilhol C, Hsiao S, Mahmoud M, Allen S, Pirri D, Ayllon BT, Akhtar S, et al. Mechanical activation of hypoxia-inducible factor

1α drives endothelial dysfunction at atheroprone sites. *Arterioscler Thromb Vasc Biol*. 2017;37:2087–2101. doi: 10.1161/ATVBAHA.117.309249
44. Wu D, Huang RT, Hamanaka RB, Krause M, Oh MJ, Kuo CH, Nigdelioglu R, Meliton AY, Witt L, Dai G, et al. HIF-1α is required for disturbed flow-induced metabolic reprogramming in human and porcine vascular endothelium. *eLife*. 2017;6:e25217.
45. Min BK, Park S, Kang HJ, Kim DW, Ham HJ, Ha CM, Choi BJ, Lee JY, Oh CJ, Yoo EK, et al. Pyruvate dehydrogenase kinase is a metabolic checkpoint for polarization of macrophages to the M1 phenotype. *Front Immunol*. 2019;10:944. doi: 10.3389/fimmu.2019.00944
46. Lundell LS, Massart J, Altıntaş A, Krook A, Zierath JR. Regulation of glucose uptake and inflammation markers by FOXO1 and FOXO3 in skeletal muscle. *Mol Metab*. 2019;20:79–88. doi: 10.1016/j.molmet.2018.09.011
47. Parsanathan R, Jain SK. Glucose-6-phosphate dehydrogenase deficiency increases cell adhesion molecules and activates human monocyte-endothelial cell adhesion: protective role of l-cysteine. *Arch Biochem Biophys*. 2019;663:11–21. doi: 10.1016/j.abb.2018.12.023
48. Wilmanski J, Siddiqi M, Deitch EA, Spolarics Z. Augmented IL-10 production and redox-dependent signaling pathways in glucose-6-phosphate dehydrogenase-deficient mouse peritoneal macrophages. *J Leukoc Biol*. 2005;78:85–94. doi: 10.1189/jlb.0105010
49. Cantelmo AR, Conradi LC, Brajic A, Goveia J, Kalucka J, Pircher A, Chaturvedi P, Hol J, Thienpont B, Teuwen LA, et al. Inhibition of the glycolytic activator PFKFB3 in endothelium induces tumor vessel normalization, impairs metastasis, and improves chemotherapy. *Cancer Cell*. 2016;30:968–985. doi: 10.1016/j.ccell.2016.10.006
50. Zhang R, Li R, Liu Y, Li L, Tang Y. The glycolytic enzyme PFKFB3 controls TNF-α-induced endothelial proinflammatory responses. *Inflammation*. 2019;42:146–155. doi: 10.1007/s10753-018-0880-x
51. Cao Y, Zhang X, Wang L, Yang Q, Ma Q, Xu J, Wang J, Kovacs L, Ayon RJ, Liu Z, et al. PFKFB3-mediated endothelial glycolysis promotes pulmonary hypertension. *Proc Natl Acad Sci USA*. 2019;116:13394-13403.
52. Tian W, Guo HS, Li CY, Cao W, Wang XY, Mo D, Hao XW, Feng YD, Sun Y, Lei F, et al. PFKFB3 promotes endotoxemia-induced myocardial dysfunction through inflammatory signaling and apoptotic induction. *Toxicol Appl Pharmacol*. 2019;368:26–36. doi: 10.1016/j.taap.2019.02.007
53. Oldham WM, Clish CB, Yang Y, Loscalzo J. Hypoxia-mediated increases in L-2-hydroxyglutarate coordinate the metabolic response to reductive stress. *Cell Metab*. 2015;22:291–303. doi: 10.1016/j.cmet.2015.06.021
54. Bertero T, Oldham WM, Grasset EM, Bourget I, Boulter E, Pisano S, Hofman P, Bellvert F, Meneguzzi G, Bulavin DV, et al. Tumor-stroma mechanics coordinate amino acid availability to sustain tumor growth and malignancy. *Cell Metab*. 2019;29:124–140.e10. doi: 10.1016/j.cmet.2018.09.012
55. Chong J, Soufan O, Li C, Caraus I, Li S, Bourque G, Wishart DS, Xia J. MetaboAnalyst 4.0: towards more transparent and integrative metabolomics analysis. *Nucleic Acids Res*. 2018;46:W486–W494. doi: 10.1093/nar/gky310
56. Xia J, Wishart DS. Web-based inference of biological patterns, functions and pathways from metabolomic data using MetaboAnalyst. *Nat Protoc*. 2011;6:743–760. doi: 10.1038/nprot.2011.319
57. Kim D, Fiske BP, Birsoy K, Freinkman E, Kami K, Possemato RL, Chudnovsky Y, Pacold ME, Chen WW, Cantor JR, et al. SHMT2 drives glioma cell survival in ischaemia but imposes a dependence on glycine clearance. *Nature*. 2015;520:363–367. doi: 10.1038/nature14363
58. Fernandez CA, Des Rosiers C, Previs SF, David F, Brunengraber H. Correction of 13C mass isotopomer distributions for natural stable isotope abundance. *J Mass Spectrom*. 1996;31:255–262. doi: 10.1002/(SICI)1096-9888(199603)31:3<255::AID-JMS290>3.0.CO;2-3
59. Antoniewicz MR. A guide to (13)C metabolic flux analysis for the cancer biologist. *Exp Mol Med*. 2018;50:19.
60. Verwer EE, Kavanagh TR, Mischler WJ, Feng Y, Takahashi K, Wang S, Shoup TM, Neelamegam R, Yang J, Guehl NJ, et al. [18F]Fluorocholine and [18F]Fluoroacetate PET as imaging biomarkers to assess phosphatidylcholine and mitochondrial metabolism in preclinical models of TSC and LAM. *Clin Cancer Res*. 2018;24:5925–5938. doi: 10.1158/1078-0432.CCR-17-3693
61. Xiao W, Sarsour EH, Wagner BA, Doskey CM, Buettner GR, Domann FE, Goswami PC. Succinate dehydrogenase activity regulates PCB3-quinone-induced metabolic oxidative stress and toxicity in HaCaT human keratinocytes. *Arch Toxicol*. 2016;90:319–332. doi: 10.1007/s00204-014-1407-3
62. Hughes EL, Cover PO, Buckingham JC, Gavins FN. Role and interactions of annexin A1 and oestrogens in the manifestation of sexual dimorphisms in cerebral and systemic inflammation. *Br J Pharmacol*. 2013;169:539–553. doi: 10.1111/j.1476-5381.2012.02146.x
63. Chen J, Lai J, Yang L, Ruan G, Chaugai S, Ning Q, Chen C, Wang DW. Trimetazidine prevents macrophage-mediated septic myocardial dysfunction via activation of the histone deacetylase sirtuin 1. *Br J Pharmacol*. 2016;173:545–561. doi: 10.1111/bph.13386
64. L'Her E, Sebert P. Effects of dichloroacetate and ubiquinone infusions on glycolysis activity and thermal sensitivity during sepsis. *J Lab Clin Med*. 2004;143:352–357. doi: 10.1016/j.lab.2004.03.004
65. Liu B, Bai W, Ou G, Zhang J. CDH1-mediated metabolic switch from pentose phosphate pathway to glycolysis contributes to sevoflurane-induced neuronal apoptosis in developing brain. *ACS Chem Neurosci*. 2019;10:2332–2344. doi: 10.1021/acschemneuro.8b00644
66. Fukumura D, Salehi HA, Witwer B, Tuma RF, Melder RJ, Jain RK. Tumor necrosis factor alpha-induced leukocyte adhesion in normal and tumor vessels: effect of tumor type, transplantation site, and host strain. *Cancer Res*. 1995;55:4824–4829.
67. Nakae J, Kitamura T, Silver DL, Accili D. The forkhead transcription factor Foxo1 (Fkhr) confers insulin sensitivity onto glucose-6-phosphatase expression. *J Clin Invest*. 2001;108:1359–1367. doi: 10.1172/JCI12876
68. Xiao W, Son J, Vorrink SU, Domann FE, Goswami PC. Ligand-independent activation of aryl hydrocarbon receptor signaling in PCB3-quinone treated HaCaT human keratinocytes. *Toxicol Lett*. 2015;233:258–266. doi: 10.1016/j.toxlet.2015.02.005
69. Dobin A, Davis CA, Schlesinger F, Drenkow J, Zaleski C, Jha S, Batut P, Chaisson M, Gingeras TR. STAR: ultrafast universal RNA-seq aligner. *Bioinformatics*. 2013;29:15–21. doi: 10.1093/bioinformatics/bts635
70. Love MI, Huber W, Anders S. Moderated estimation of fold change and dispersion for RNA-seq data with DESeq2. *Genome Biol*. 2014;15:550. doi: 10.1186/s13059-014-0550-8
71. Cornwell M, Vangala M, Taing L, Herbert Z, Köster J, Li B, Sun H, Li T, Zhang J, Qiu X, et al. VIPER: visualization pipeline for RNA-seq, a Snakemake workflow for efficient and complete RNA-seq analysis. *BMC Bioinformatics*. 2018;19:135. doi: 10.1186/s12859-018-2139-9